

Supporting information for

**Heterometallic Calcium–Alkali Metal Aryloxides as Catalysts for the  
Solvothermal Alcoholysis of Nylon-6 Waste**

Rafał Petrus,<sup>1,\*</sup> Karolina Matuszak,<sup>1</sup> Adrian Kowaliński,<sup>1</sup> and Tadeusz Lis<sup>2</sup>

<sup>1</sup> Faculty of Chemistry, Wrocław University of Science and Technology,

23 Smoluchowskiego, 50-370 Wrocław, Poland

<sup>2</sup> Faculty of Chemistry, University of Wrocław, 14 F. Joliot-Curie, 50-383 Wrocław, Poland.

\*Corresponding author email: [rafal.petrus@pwr.edu.pl](mailto:rafal.petrus@pwr.edu.pl)

Contents

Chemical recycling of polyamide 6 (PA6).....	S2
X-Ray Crystallography of <b>1-9</b> .....	S5
Continuous-shape measurements of the coordination environment around metal ions in <b>1-9</b> .....	S7
Molecular structures of <b>8-9</b> .....	S8
IR, <sup>1</sup> H and <sup>13</sup> C NMR spectra of <b>1-9</b> .....	S9
<sup>1</sup> H DOSY NMR spectra of <b>1-8</b> .....	S23
FTIR-ATR, NMR, and ESI-MS spectra of organic products obtained by chemical depolymerization of PA6 using MeOH.....	S30
FTIR-ATR, NMR, and ESI-MS spectra of organic products obtained by chemical depolymerization of PA6 using BnOH.....	S35
Summary of alcoholysis of PA6, using MeOH in the presence of <b>2-21</b> at 200-240 °C.....	S37
Summary of alcoholysis of PA6, using BnOH in the presence of <b>2-6</b> and <b>10-21</b> at 260 °C.....	S39

## Chemical recycling of polyamide 6 (PA6)

Polyamides (PAs) are an important group of thermoplastic polymers widely used in household and engineering applications. Among them, polyamide 6 (PA6) is the most commonly utilized due to its high heat and mechanical resistance, high tensile strength, and excellent chemical resistance to acids and alkalis. These properties make it suitable for various applications, including construction, automotive, textiles, and separation processes.<sup>1,2</sup> However, due to its excellent chemical and thermal stability, recycling post-consumer PA6 presents a significant challenge. Mechanical recycling is a common method for PA6 recycling because of its lower cost, shorter processing time, reduced carbon footprint, and lower environmental impact. However, it often results in degradation and deterioration of the material's properties.<sup>3</sup> In contrast, chemical recycling breaks down the polymer chain into monomers, oligomers, or other low-molecular-weight derivatives, making it a viable option for plastics that are no longer suitable for mechanical recycling.<sup>4</sup> As a result, there is a growing interest in developing and improving closed-loop recycling processes for post-consumer PA6 waste.<sup>5</sup> Various chemical depolymerization routes have been explored for PAs, including pyrolysis, hydrolysis, hydrogenolysis, ammonolysis, aminolysis, and alcoholysis. Generally, PA6 chemical recycling requires high temperatures (270–320 °C), high-pressure steam, long reaction times, sub- and supercritical water/ammonia/amines/alcohols, acid or base reagents, and efficient catalysts (e.g., inorganic acids, organic acids/bases, metal salts, or hydroxides).<sup>6-9</sup> Most studies focus on PA6 depolymerization to recover  $\epsilon$ -caprolactam (CL), the cyclic monomer, which is subsequently isolated via distillation.

Solvent-free depolymerization of PA6 at 375 °C over  $\alpha$ -Al<sub>2</sub>O<sub>3</sub>@KOH in a fluidized bed reactor or at 250 °C under 400 Pa using NaOH enables the recovery of CL with yields of 85–90% in less than 3 minutes,<sup>10</sup> or 90% after 4.5 hours, respectively.<sup>11</sup> Heating a mixture of

PA6 and 5 mol%  $\text{La}(\text{N}(\text{SiMe}_3)_2)_3$  in a sealed cylindrical Schlenk flask at 240 °C for 4 h under 0.133 Pa vacuum results in 90% polymer conversion to CL.<sup>12</sup> Treatment of PA6 in an ionic liquid at 300 °C using 5 wt% DMP yields CL with 70–86% efficiency after 6 h.<sup>13,14</sup> AlliedSignal Inc. developed an efficient process for recovering 90–95% of CL from PA6-containing waste through thermal degradation at 300–340 °C and pressures of 0.60–1.43 MPa using superheated steam at a rate of 3–6 g/min over 3–6 h.<sup>15</sup> BASF Corporation investigated the continuous and semi-continuous recovery of CL from PA6 carpet using  $\text{H}_3\text{PO}_4$  (5–25 wt%) and steam at 230–325 °C.<sup>16,17</sup> Hydrolysis of PA6 in subcritical water allows for 90–92% CL recovery at 300 °C within 1 h, using a reagent mass ratio of PA6/ $\text{H}_2\text{O}$  = 1/11.<sup>18</sup> Microwave irradiation (200 W) of PA6 hydrolysis for 15 minutes with  $\text{H}_3\text{PO}_4$  (PA6/ $\text{H}_2\text{O}/\text{H}_3\text{PO}_4$  = 1/6.3/0.8) produces a mixture consisting of over 90%  $\epsilon$ -aminocaproic acid and its linear oligomers, along with minor cyclic products.<sup>19</sup> Complete depolymerization of PA6 via microwave-assisted reaction with  $\text{Ac}_2\text{O}$  at 260 °C for 15 minutes, using an organic base with  $\text{Zn}(\text{OAc})_2$  or  $\text{Sn}(\text{Oct})_2$  as catalysts (PA6/ $\text{Ac}_2\text{O}$ /cat. = 1/5/0.05), results in a product mixture containing approximately 70% N-acylated  $\epsilon$ -caprolactam.<sup>20</sup> DuPont's 1994 patent describes the ammonolysis of a PA66 and PA6 mixture (1:1 wt) at 330 °C for 90 minutes at 13.9 MPa, using  $(\text{NH}_4)_2\text{HPO}_4$  (3.33 wt%) to recover a broad monomer mixture: PA66 components include hexamethylene diamine (72%), adiponitrile (52%), and 5-cyanovaleramide (5%); PA6 components include 6-aminocapronitrile (70%), CL (27%), and 6-aminocaproamide (1%).<sup>21</sup> DSM NV used a similar method to recover 70% of CL by aminolysis at 315–330 °C for 2 h using  $(\text{NH}_4)_2\text{HPO}_4$  (10 wt%) and  ${}^n\text{PrNH}_2$  (132 g/h).<sup>22</sup> PA6 has also been hydrogenatively depolymerized with 77–80% efficiency at 150 °C using  $\text{H}_2$  (70 bar, DMSO, 2 mol% ruthenium pincer catalyst, 8 mol%  $\text{KOtBu}$ , 48 h), yielding 24–26% of 6-amino-1-hexanol.<sup>23</sup> Ethylene glycol and  $\text{H}_3\text{PO}_4$  enable PA6 recycling at 250 °C for 45 minutes (PA6/EG/ $\text{H}_3\text{PO}_4$  = 1/6.2/0.1), leading to linear oligomers esterified with EG and N-

alkyl derivatives of CL.<sup>24</sup> Another approach involves using supercritical secondary or tertiary alcohols to convert PA6 into CL with 93–97% efficiency at 370 °C after 1.5 h (PA6/ROH = 1/13.33 wt). Under the same conditions, primary alcohols (MeOH, EtOH, <sup>n</sup>PrOH, <sup>n</sup>BuOH) enable the recovery of 14–47% CL, with yields increasing as the alcohol's alkyl chain lengthens.<sup>25</sup> Depolymerization of PA6 with supercritical MeOH at 300–370 °C produces CL, N-methylcaprolactam, methyl 6-hydroxycaproate, methyl 5-hexenoate, and methyl 6-(N,N-dimethylamino)caproate, with total yields of 77–81%.<sup>26</sup> Methanolysis of PA6 in the presence of 5 equivalents of glycolic acid at 270 °C for 6 h yields methyl 6-hydroxycaproate (67%) and methyl 5-hexenoate (11%).<sup>6</sup>

### Crystallographic Data for Compounds 1-9.

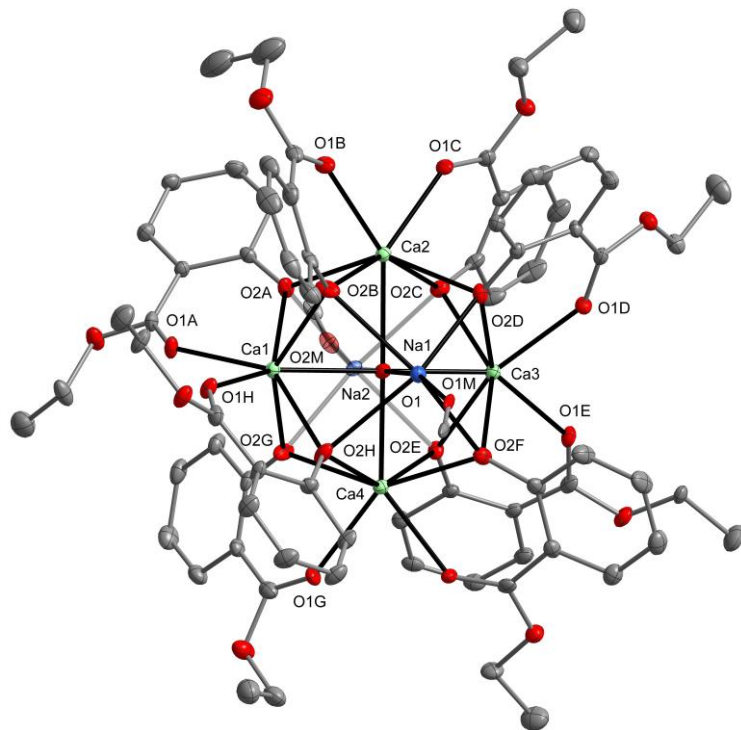
**Table S1.** Crystal and data collection parameters for compounds **1-9**.

Crystal	<b>1</b>	<b>2·1.74(THF) ·0.26(MeOH)</b>	<b>3·2a·2(THF)</b>	<b>4</b>
Chemical formula	C <sub>17</sub> H <sub>18</sub> CaO <sub>7</sub>	C <sub>57.23</sub> H <sub>64.97</sub> Ca <sub>3</sub> O <sub>22</sub> ·C <sub>56</sub> H <sub>58</sub> Ca <sub>2</sub> Li <sub>2</sub> O <sub>20</sub>	C <sub>64</sub> H <sub>74</sub> Ca <sub>3</sub> O <sub>22</sub> ·C <sub>56</sub> H <sub>58</sub> Ca <sub>2</sub> Na <sub>2</sub> O <sub>22</sub>	C <sub>52</sub> H <sub>58</sub> Ca <sub>2</sub> Na <sub>2</sub> O <sub>22</sub>
Formula Mass	374.39	1225.01	2604.74	1161.12
Crystal system	Orthorhombic	Triclinic	Triclinic	Monoclinic
Space group	<i>Pnna</i>	<i>P\bar{1}</i>	<i>P\bar{1}</i>	<i>P2<sub>1</sub>/c</i>
<i>a</i> /Å	7.1400(13)	10.522(3)	12.0381(5)	13.359(3)
<i>b</i> /Å	23.016(3)	12.290(3)	12.0786(5)	16.571(2)
<i>c</i> /Å	9.9660(15)	12.746(3)	21.7250(8)	27.326(3)
$\alpha/^\circ$		103.98(3)	86.235(3)	
$\beta/^\circ$		97.10(2)	80.894(3)	118.09(2)
$\gamma/^\circ$		105.23(2)	83.391(3)	
Unit cell volume/Å <sup>3</sup>	1637.8(4)	1512.1(7)	3094.7(2)	5336.7(17)
Temperature/K	100(2)	100(2)	100(2)	100(2)
<i>Z</i>	4	1	1	4
Radiation type	CuKα	MoKα	MoKα	MoKα
Absorption coefficient, $\mu/\text{mm}^{-1}$	3.656	0.349	0.305	0.312
No. of reflections measured	6598	11034	26696	13234
No. of independent reflections	1468	6507	13317	13234
No. of observed reflections ( $I > 2\sigma(I)$ )	1359	5211	10049	9935
$R_{int}$	0.0271	0.0239	0.0586	
Final $R_I$ values ( $I > 2\sigma(I)$ )	0.0272	0.0530	0.0734	0.1008
Final $wR(F^2)$ values ( $I > 2\sigma(I)$ )	0.0721	0.1343	0.1977	0.2671
Final $R_I$ values (all data)	0.0295	0.0684	0.0950	0.1259
Final $wR(F^2)$ values (all data)	0.0743	0.1502	0.2275	0.2778
Goodness of fit on $F^2$	1.057	1.035	1.048	1.125
$\Delta\rho_{\text{max}}/\text{e}\text{\AA}^{-3}$	0.344	0.589	1.275	1.436
$\Delta\rho_{\text{min}}/\text{e}\text{\AA}^{-3}$	-0.236	-0.596	-1.099	-1.449

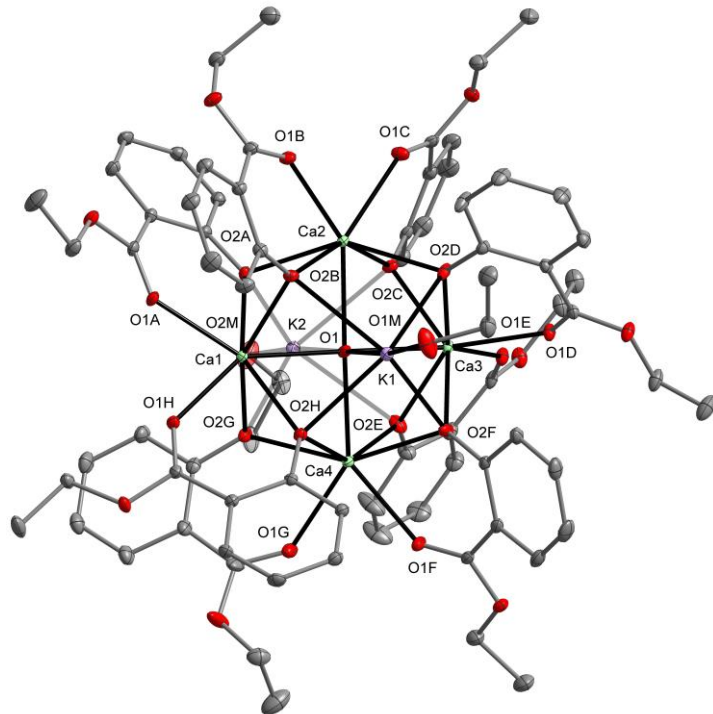
Crystal	<b>6</b>	<b>7·C<sub>7</sub>H<sub>8</sub></b>	<b>8</b>	<b>9</b>
Chemical formula	C <sub>64</sub> H <sub>56</sub> CaLi <sub>6</sub> O <sub>24</sub>	C <sub>108</sub> H <sub>110</sub> Ca <sub>3</sub> Na <sub>4</sub> O <sub>36</sub>	C <sub>73</sub> H <sub>77</sub> Ca <sub>4</sub> NaO <sub>26</sub>	C <sub>74</sub> H <sub>79</sub> Ca <sub>4</sub> KO <sub>26</sub>
Formula Mass	1290.80	2288.29	1553.65	1583.79
Crystal system	Triclinic	Monoclinic	Triclinic	Triclinic
Space group	<i>P</i> ī	<i>C</i> 2/c	<i>P</i> ī	<i>P</i> ī
<i>a</i> /Å	11.710(2)	30.627(11)	12.992(4)	13.086(2)
<i>b</i> /Å	12.320(2)	13.536(4)	14.402(6)	13.971(3)
<i>c</i> /Å	13.076(3)	55.88(2)	21.140(8)	22.268(5)
$\alpha/^\circ$	75.53(2)		76.62(5)	72.93(3)
$\beta/^\circ$	64.48(2)	99.16(5)	82.23(4)	80.83(2)
$\gamma/^\circ$	73.31(2)		77.37(5)	75.27(3)
Unit cell volume/Å <sup>3</sup>	1613.2(6)	22871(14)	3740(3)	3748.0(15)
Temperature/K	100(2)	100(2)	100(2)	100(2)
<i>Z</i>	1	8	2	2
Radiation type	MoKα	MoKα	MoKα	MoKα
Absorption coefficient, $\mu/\text{mm}^{-1}$	0.177	0.241	0.375	0.425
No. of reflections measured	19134	64014	28017	56536
No. of independent reflections	7024	23135	15528	16294
No. of observed reflections ( $I > 2\sigma(I)$ )	6183	11402	6843	11493
$R_{int}$	0.0367	0.0930	0.0673	0.0934
Final $R_I$ values ( $I > 2\sigma(I)$ )	0.0444	0.1016	0.0684	0.0584
Final $wR(F^2)$ values ( $I > 2\sigma(I)$ )	0.1191	0.2333	0.1211	0.1432
Final $R_I$ values (all data)	0.0497	0.1888	0.1836	0.0896
Final $wR(F^2)$ values (all data)	0.1263	0.2911	0.1634	0.1686
Goodness of fit on $F^2$	1.045	1.053	0.967	1.056
$\Delta\rho_{\max}/\text{e}\text{\AA}^{-3}$	0.408	0.631	0.617	0.472
$\Delta\rho_{\min}/\text{e}\text{\AA}^{-3}$	-0.338	-0.937	-0.411	-0.572

**Table S2.** Continuous-shape measurements (CShM) of the coordination environment around calcium ions in **1–9**.

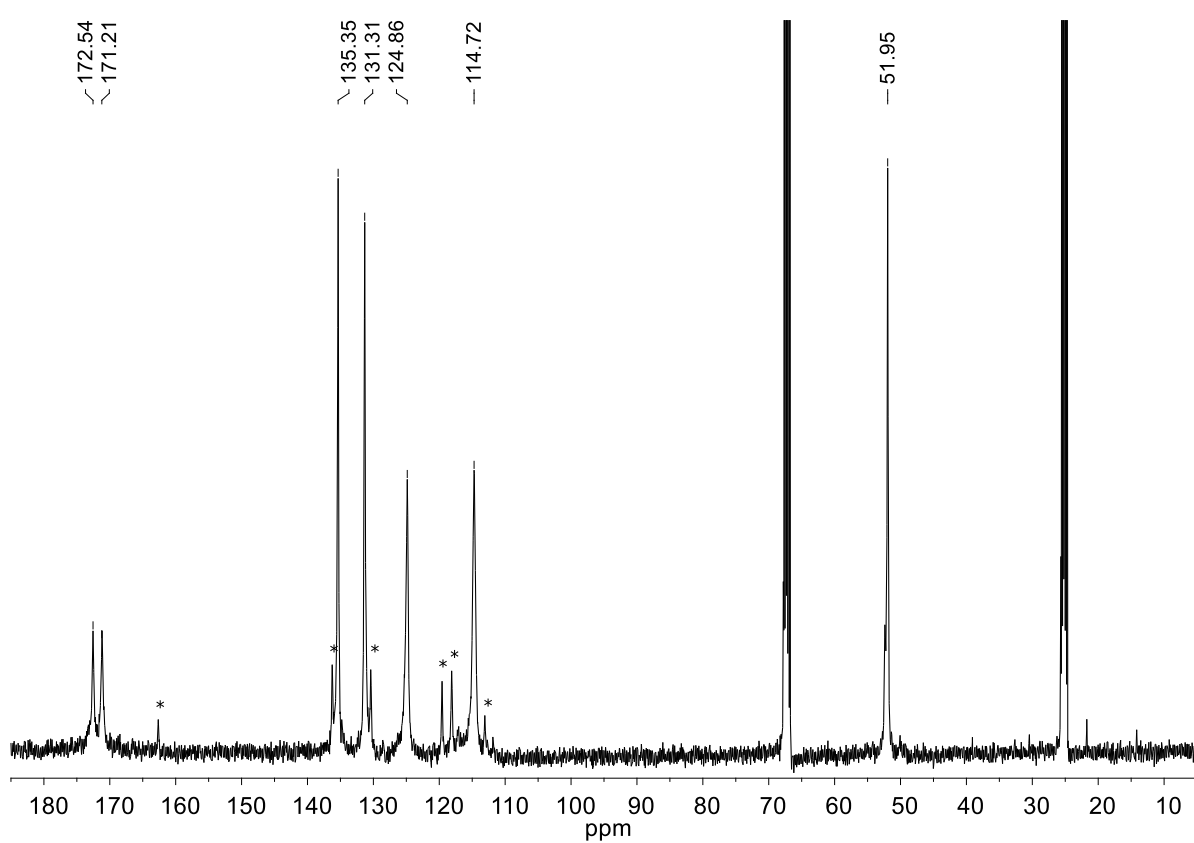
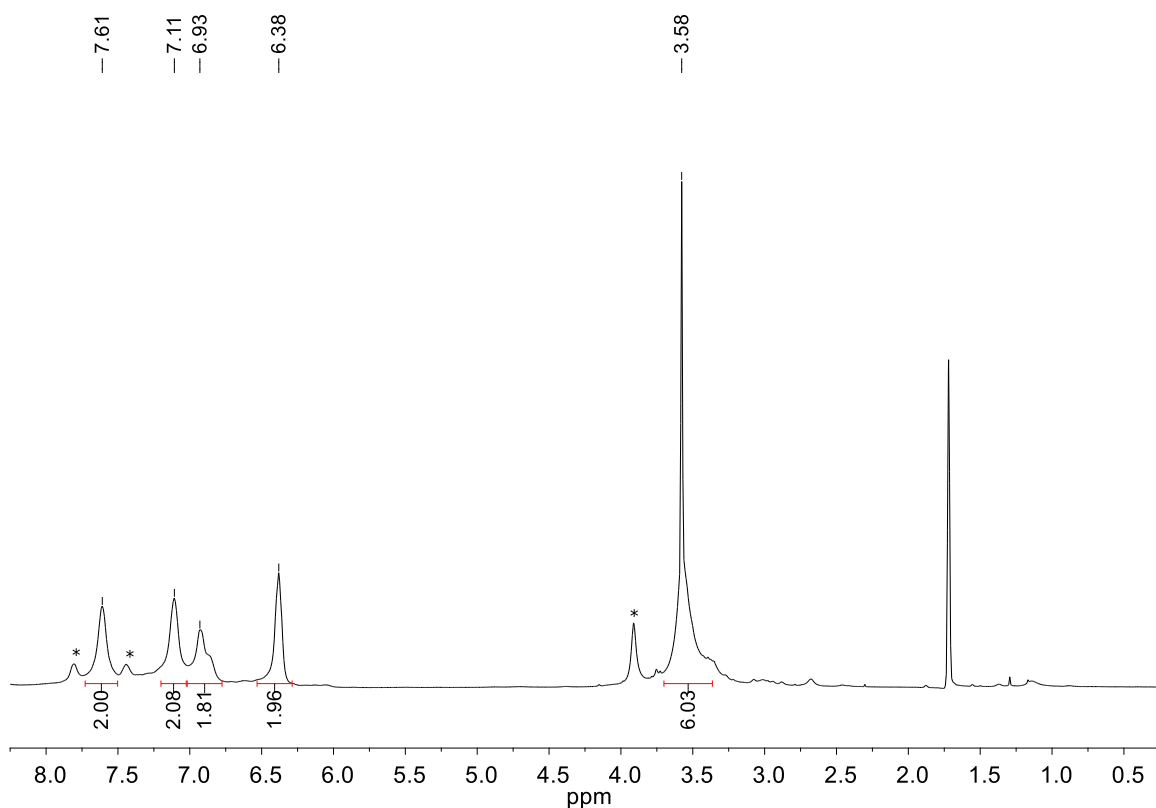
compound	atom	donor atoms	polyhedron	S parameter
<b>1</b>	Ca1	O <sub>7</sub>	capped trigonal prism	1.834
	Ca1	O <sub>7</sub>	capped trigonal prism	1.060
<b>2</b>	Ca2	O <sub>6</sub>	octahedron	2.408
	Ca2	O <sub>8</sub>	triangular dodecahedron	0.969
<b>2a</b>	Ca3	O <sub>6</sub>	octahedron	2.797
	Ca1	O <sub>7</sub>	capped trigonal prism	1.212
<b>3</b>	Li1	O <sub>4</sub>	axially vacant trigonal bipyramid	0.748
	Ca1	O <sub>7</sub>	capped trigonal prism	0.742
<b>4</b>	Ca2	O <sub>7</sub>	capped trigonal prism	0.776
	Na1	O <sub>5</sub>	vacant octahedron	2.779
	Na2	O <sub>5</sub>	vacant octahedron	2.334
	Ca1	O <sub>6</sub>	octahedron	2.188
<b>6</b>	Li1	O <sub>4</sub>	axially vacant trigonal bipyramid	2.084
	Li2	O <sub>4</sub>	axially vacant trigonal bipyramid	2.122
	Li3	O <sub>5</sub>	trigonal bipyramid	1.874
	Ca1	O <sub>8</sub>	square antiprism	0.978
<b>7</b>	Ca2	O <sub>6</sub>	octahedron	3.522
	Ca3	O <sub>5</sub>	octahedron	3.271
	Na1	O <sub>6</sub>	trigonal prism	7.174
	Na2	O <sub>6</sub>	octahedron	6.309
	Na3	O <sub>6</sub>	octahedron	6.891
	Na4	O <sub>6</sub>	octahedron	6.649
	Ca1	O <sub>7</sub>	capped trigonal prism	1.012
<b>8</b>	Ca2	O <sub>7</sub>	capped trigonal prism	1.024
	Ca3	O <sub>7</sub>	capped trigonal prism	1.386
	Ca4	O <sub>7</sub>	capped trigonal prism	1.180
	Na1	O <sub>6</sub>	octahedron	3.570
	Na2	O <sub>6</sub>	octahedron	3.547
	Ca1	O <sub>7</sub>	capped trigonal prism	1.586
<b>9</b>	Ca2	O <sub>7</sub>	capped trigonal prism	0.770
	Ca3	O <sub>7</sub>	capped trigonal prism	0.752
	Ca4	O <sub>7</sub>	capped trigonal prism	0.993
	K1	O <sub>6</sub>	octahedron	6.919
	K2	O <sub>6</sub>	octahedron	6.771

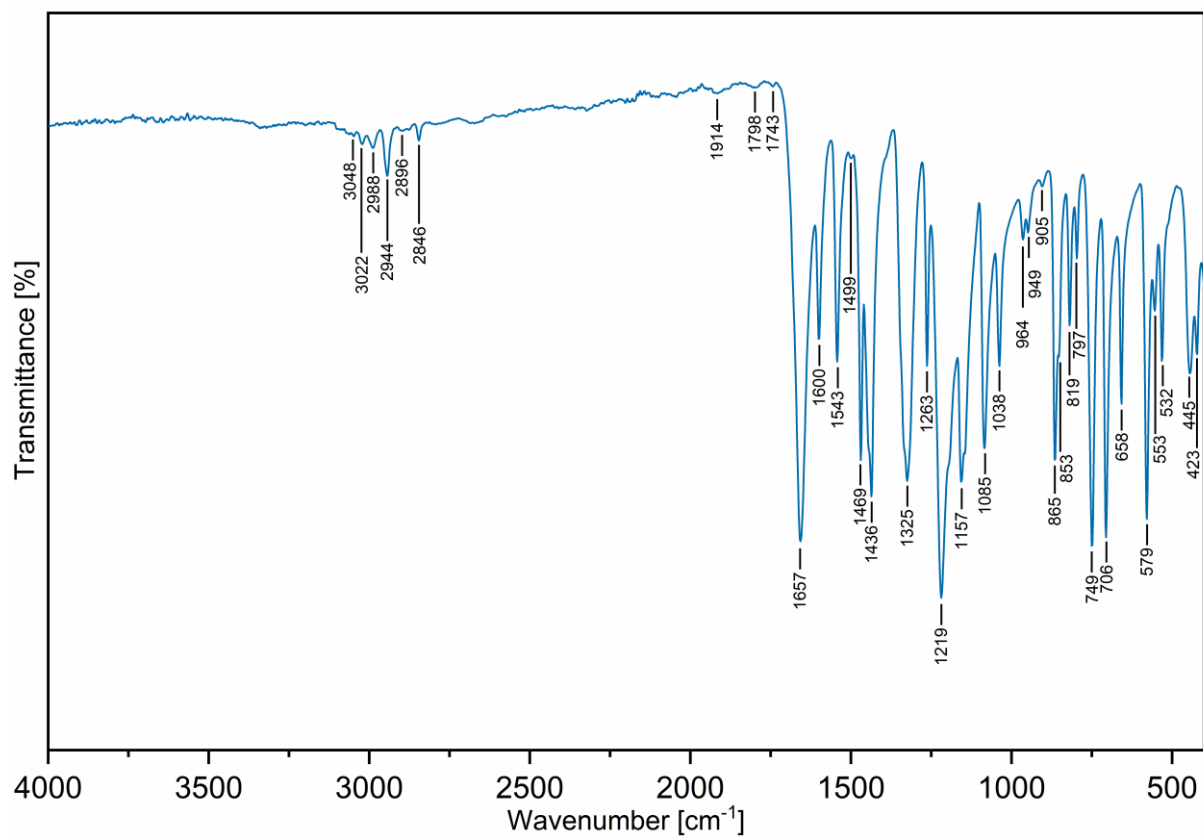


**Figure S1.** The molecular structure of  $[\text{Ca}_4\text{Na}(\mu_5\text{-OH})(\text{sal-Et})_8(\text{MeOH})]$  (**8**). The displacement ellipsoids are drawn at the 25% probability level. Hydrogen atoms have been omitted for the sake of clarity.

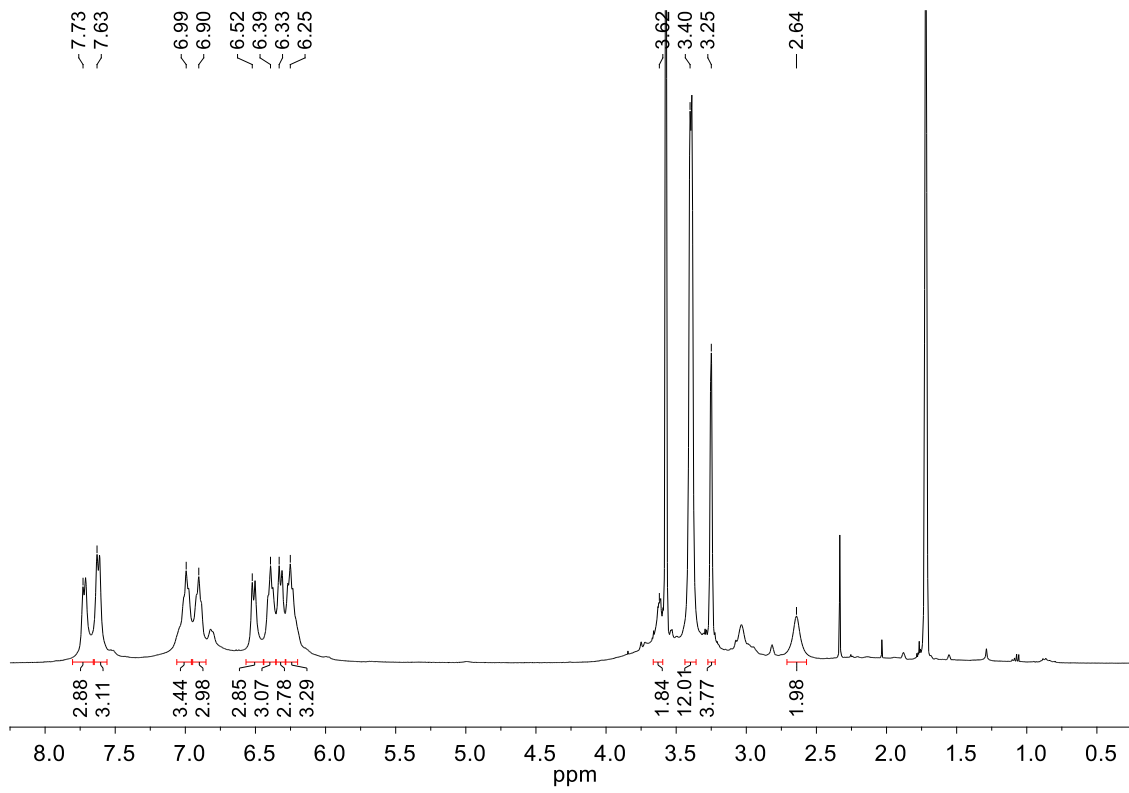


**Figure S2.** The molecular structure of  $[\text{Ca}_4\text{K}(\mu_5\text{-OH})(\text{sal-Et})_8(\text{EtOH})]$  (**9**). The displacement ellipsoids are drawn at the 25% probability level. Hydrogen atoms have been omitted for the sake of clarity.

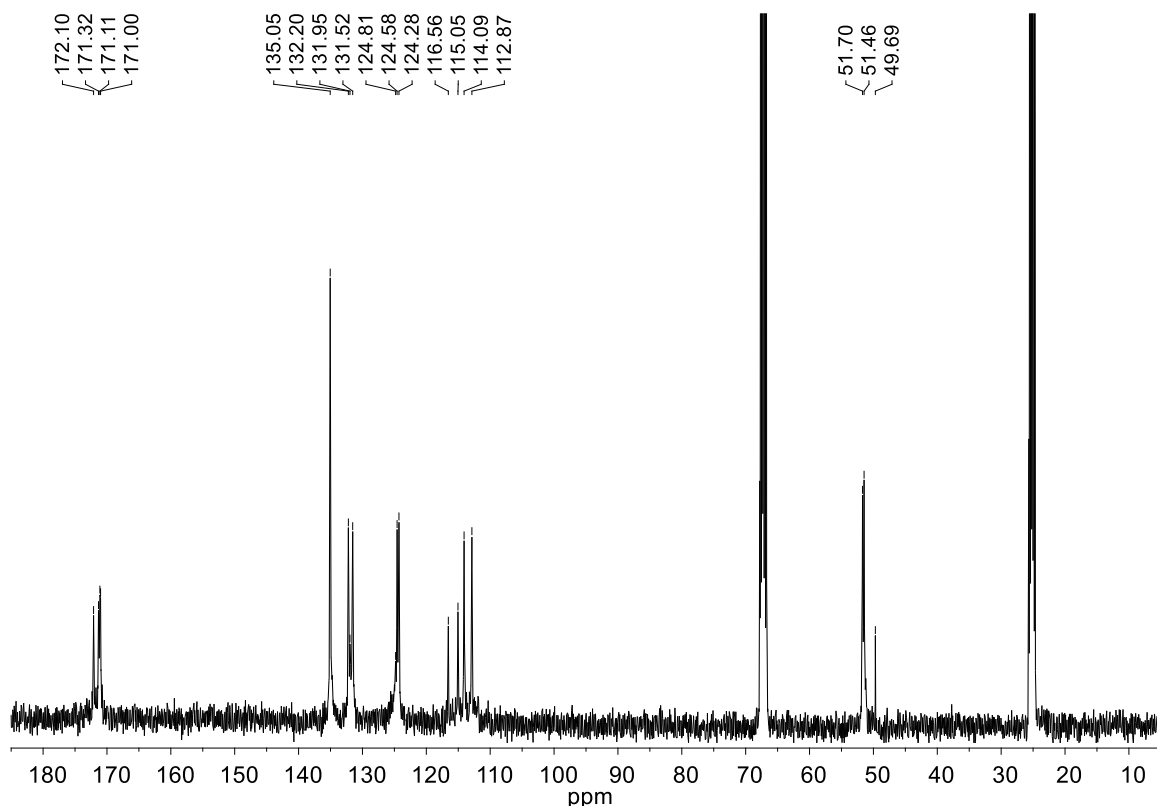




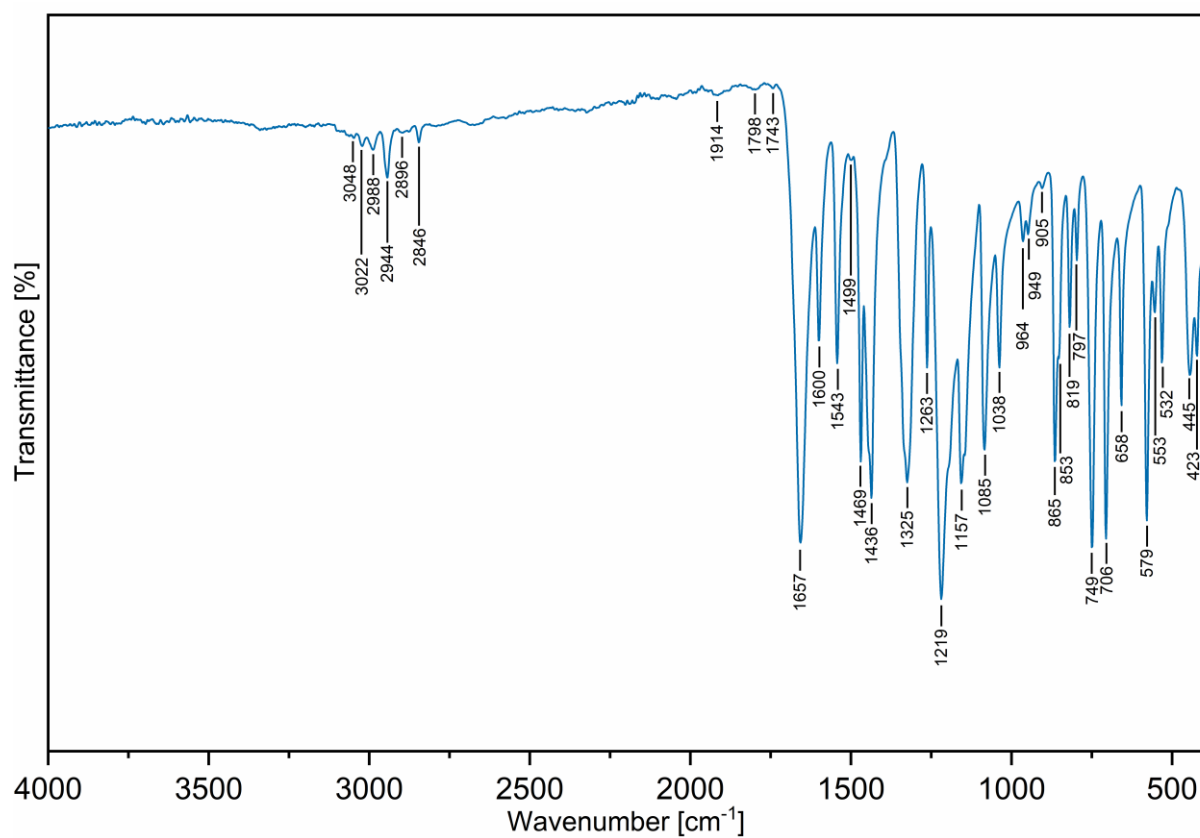
**Figure S5.** FTIR-ATR spectrum of **1**.



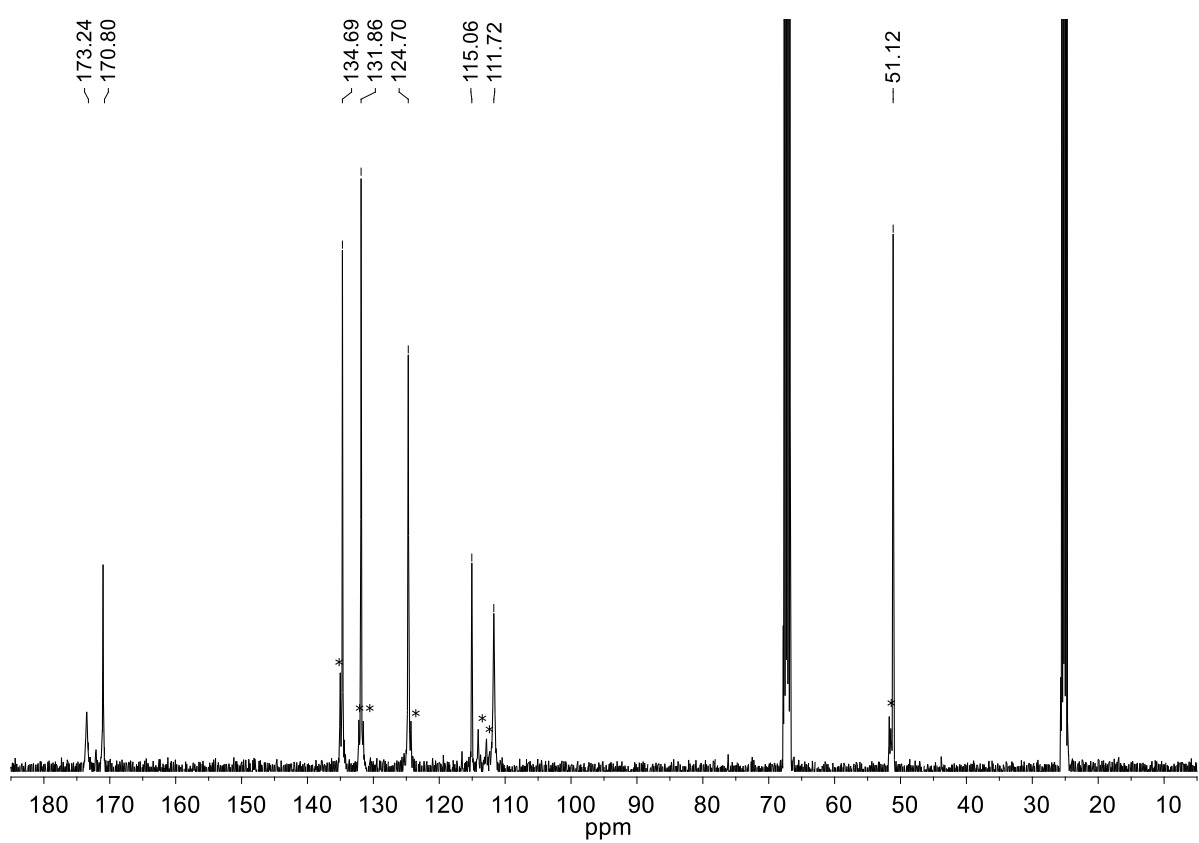
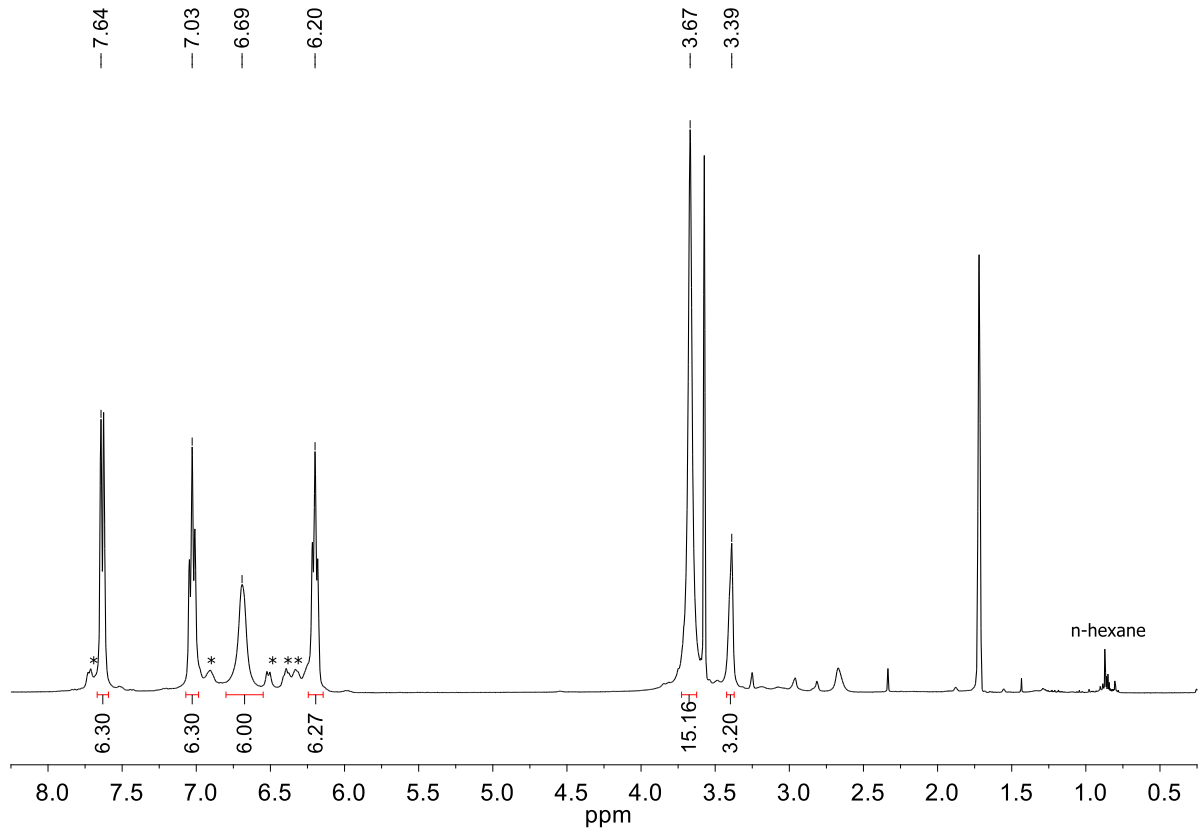
**Figure S6.**  $^1\text{H}$  NMR spectrum of **2** in  $\text{THF-d}_8$ .



**Figure S7.**  $^{13}\text{C}$  NMR spectrum of **2** in  $\text{THF-d}_8$ .



**Figure S8.** FTIR-ATR spectrum of **2**.



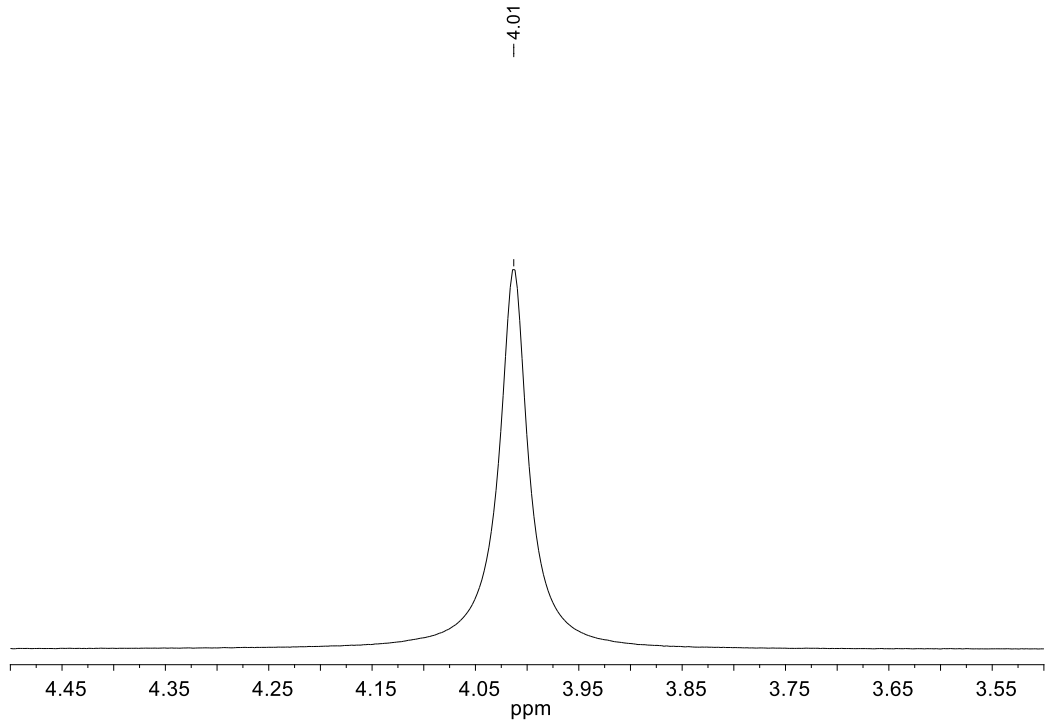


**Figure S11.** <sup>7</sup>Li NMR spectrum of **3**.

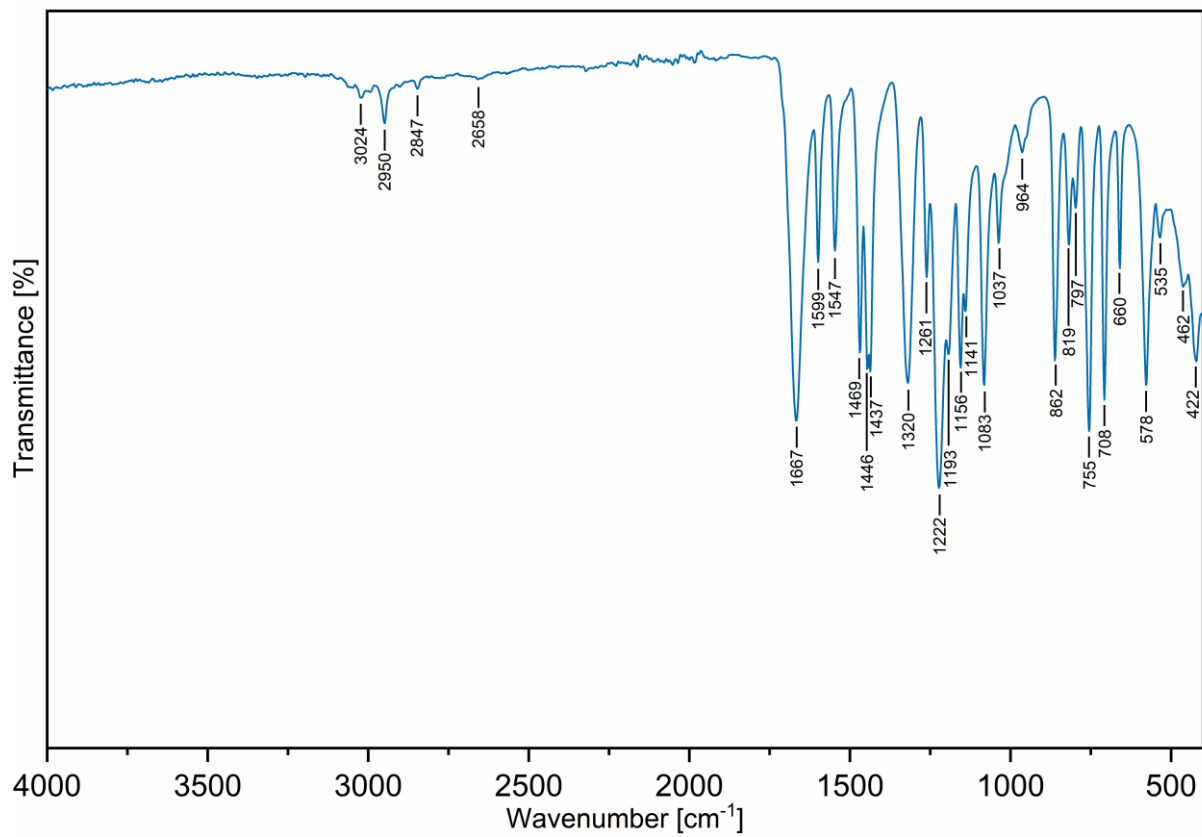


**Figure S12.** FTIR-ATR spectrum of **3**.

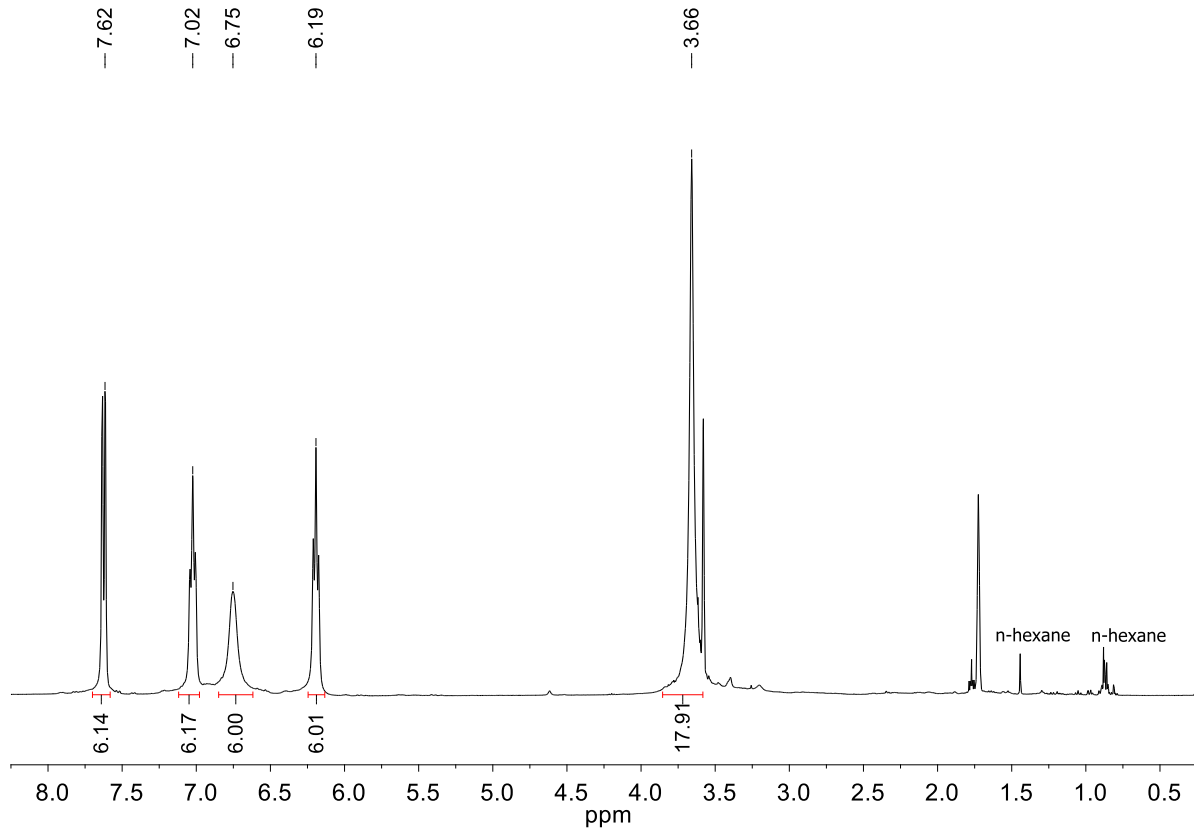


**Figure S13.** <sup>1</sup>H NMR spectrum of **4** in THF-d<sub>8</sub>.

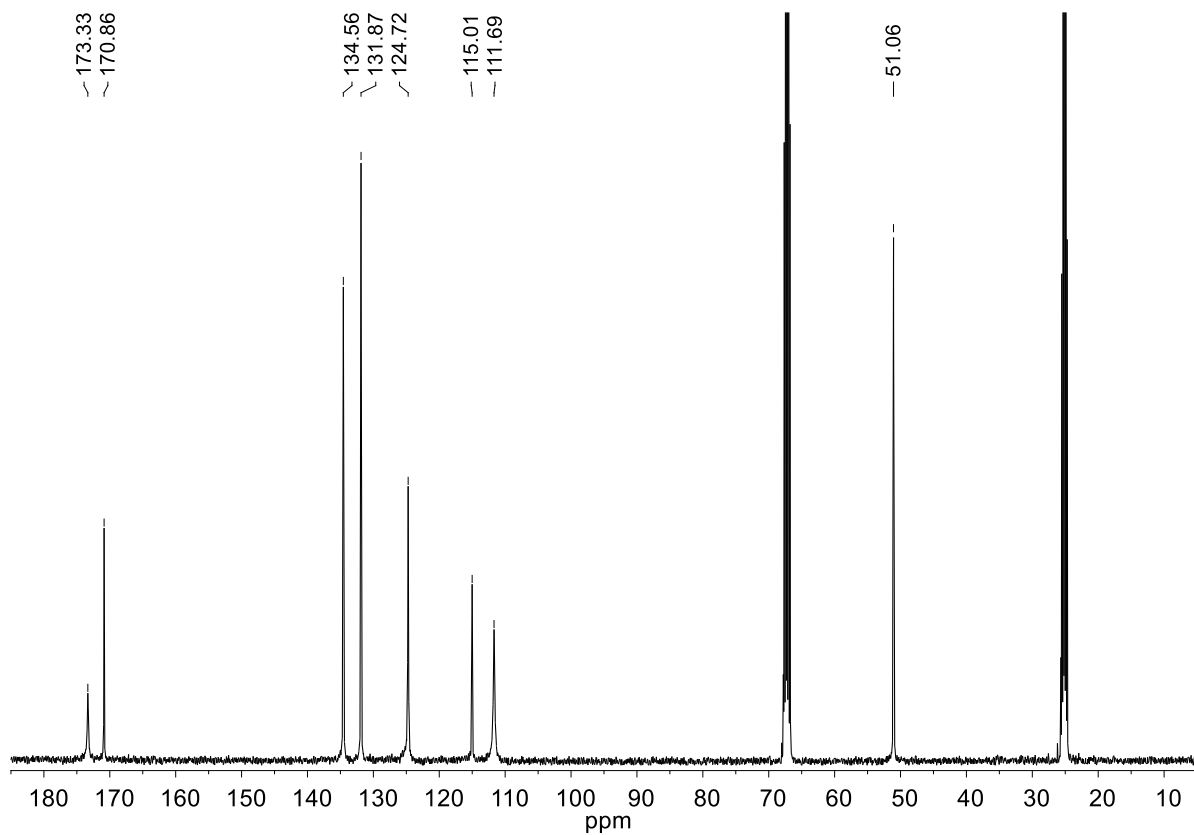


**Figure S14.** <sup>13</sup>C NMR spectrum of **4** in THF-d<sub>8</sub>.

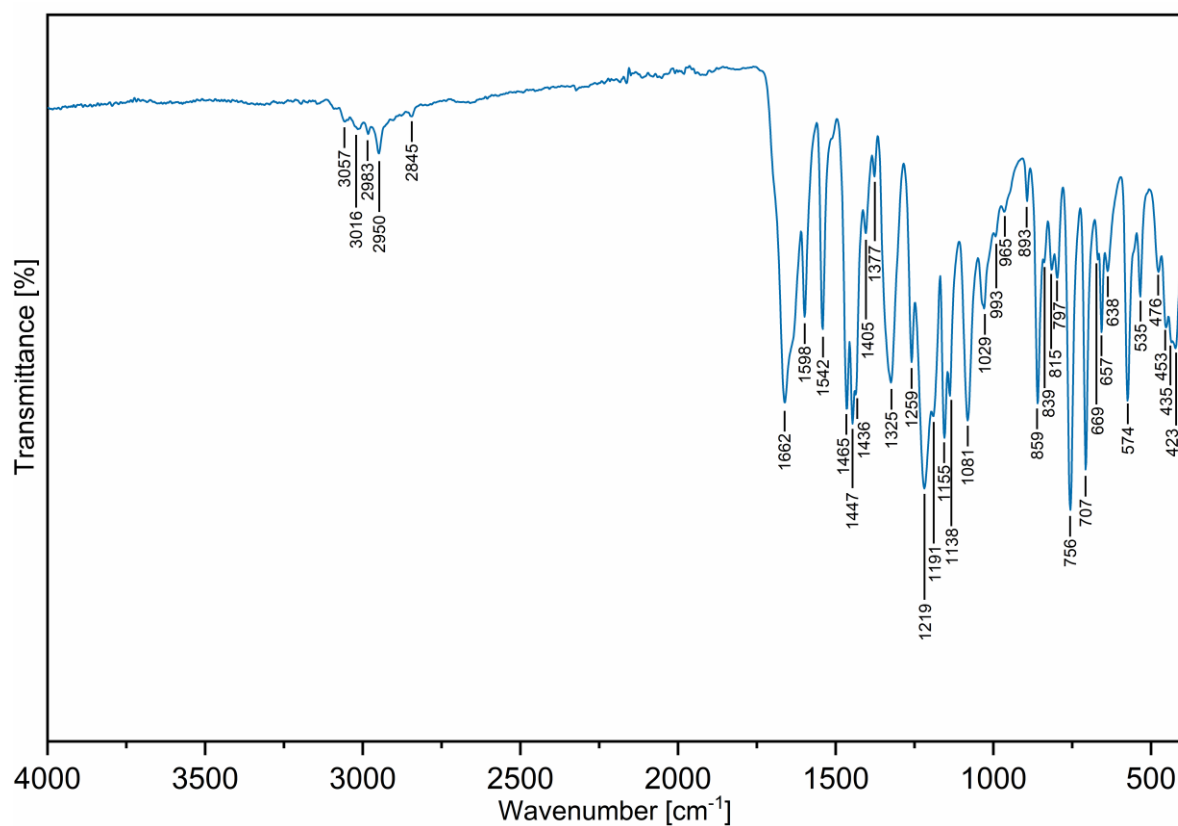


**Figure S15.** FTIR-ATR spectrum of **4**.

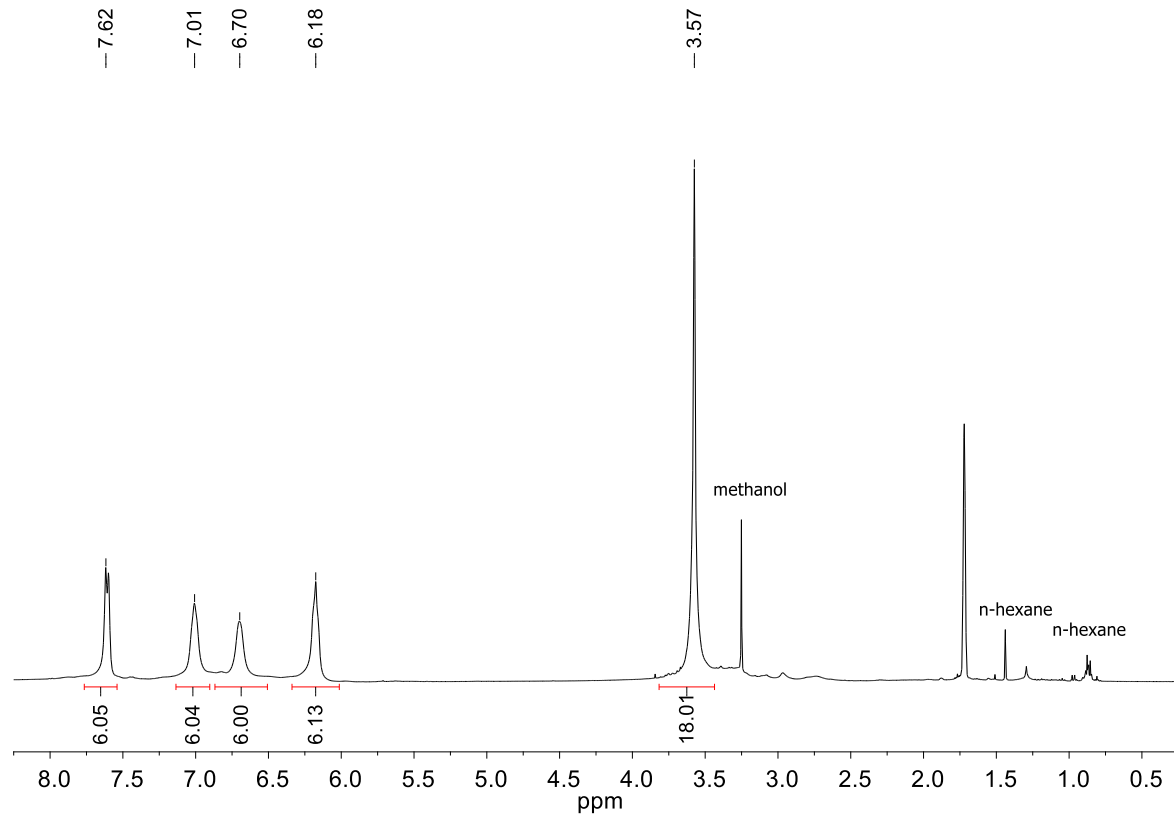


**Figure S16.**  $^1\text{H}$  NMR spectrum of **5** in  $\text{THF-d}_8$ .

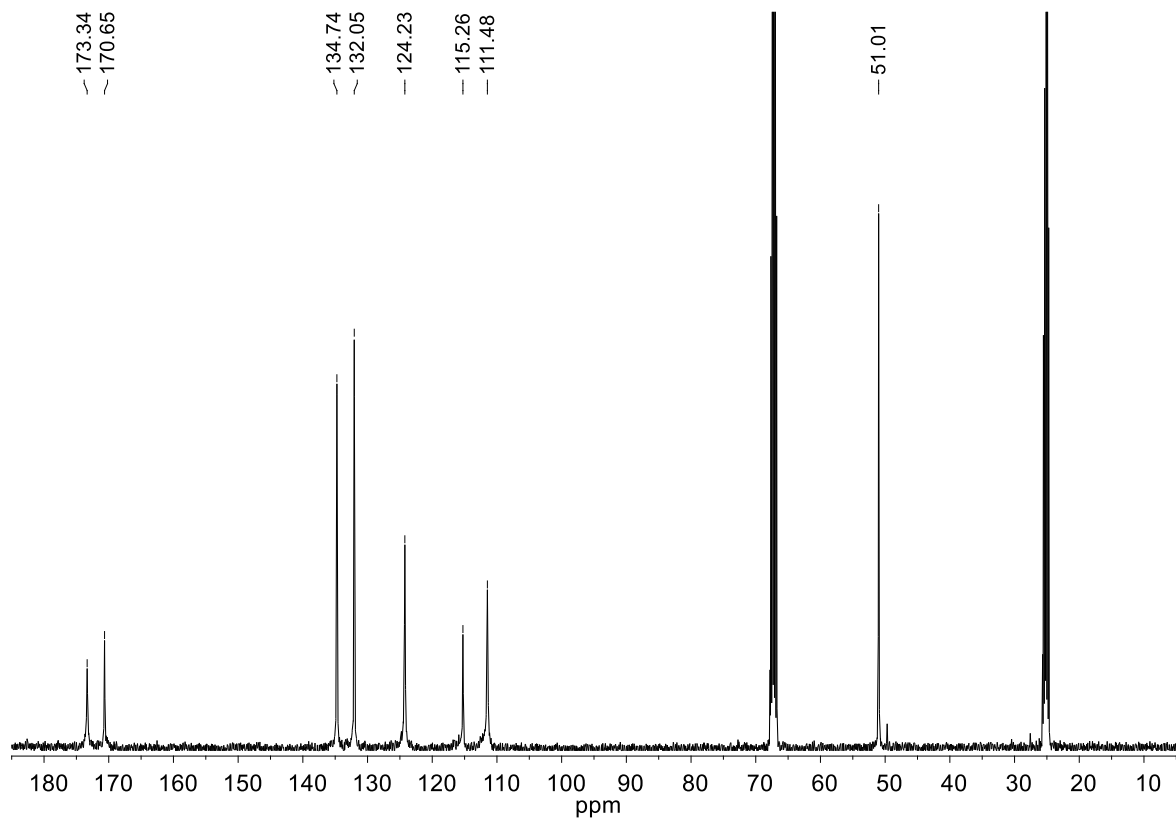


**Figure S17.**  $^{13}\text{C}$  NMR spectrum of **5** in  $\text{THF-d}_8$ .

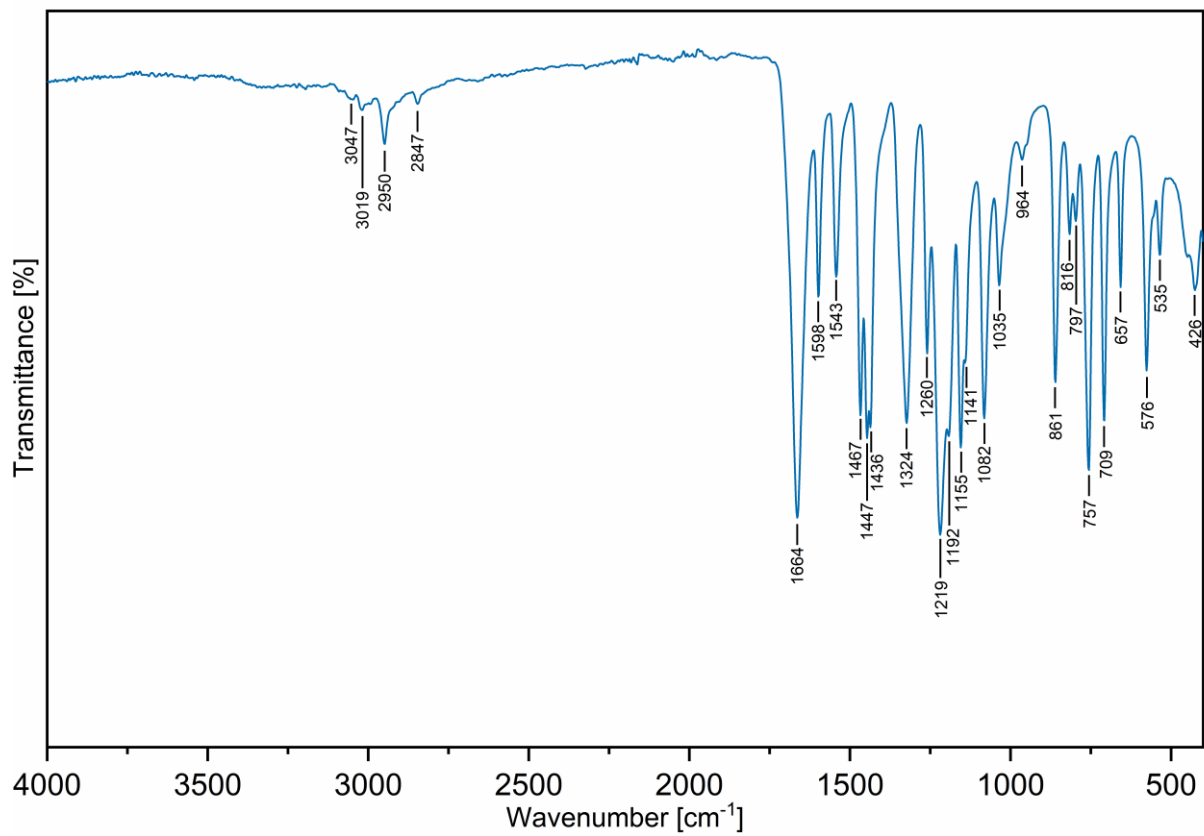


**Figure S18.** FTIR-ATR spectrum of **5**.

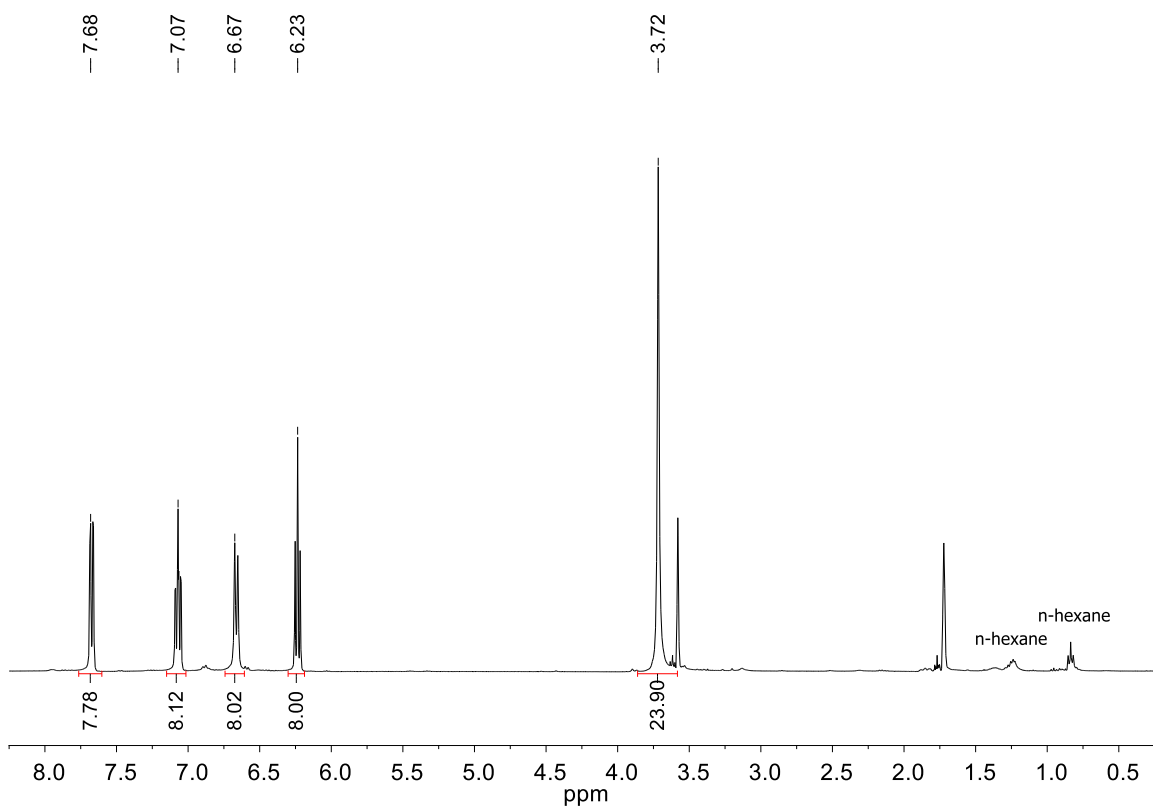


**Figure S19.** <sup>1</sup>H NMR spectrum of **6** in THF-d<sub>8</sub>.

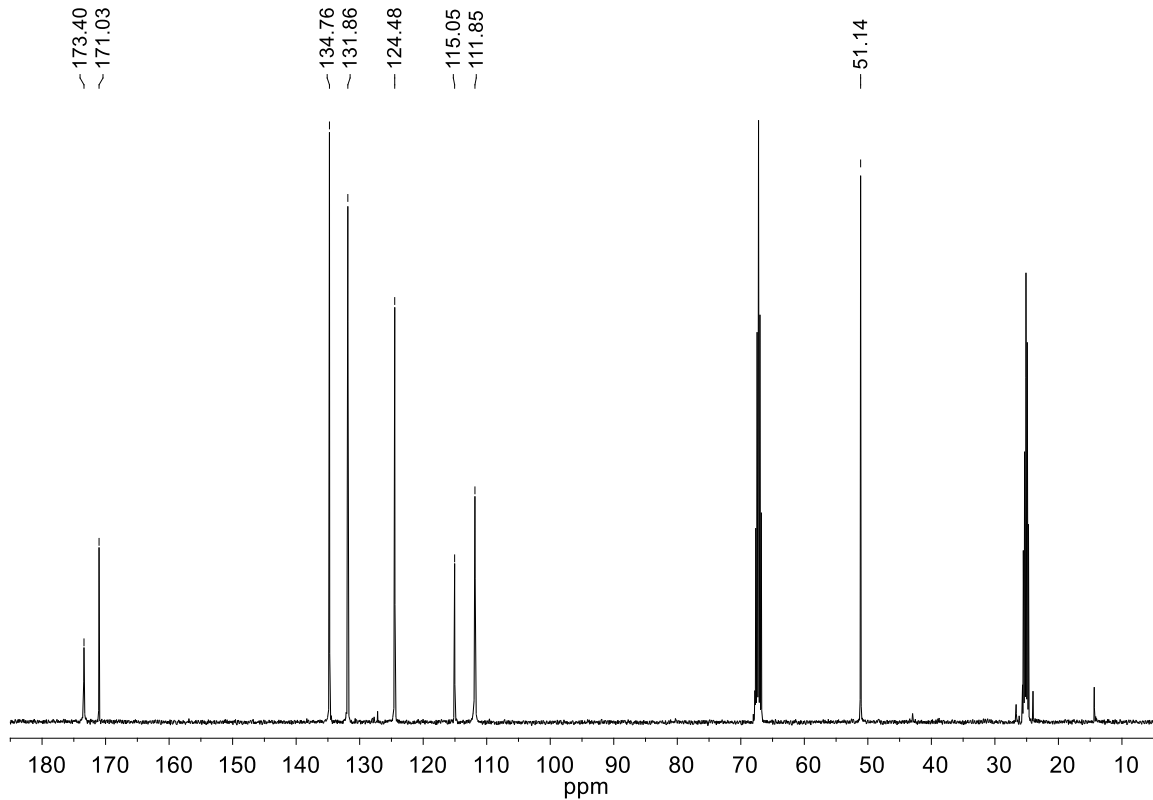


**Figure S20.** <sup>13</sup>C NMR spectrum of **6** in THF-d<sub>8</sub>.

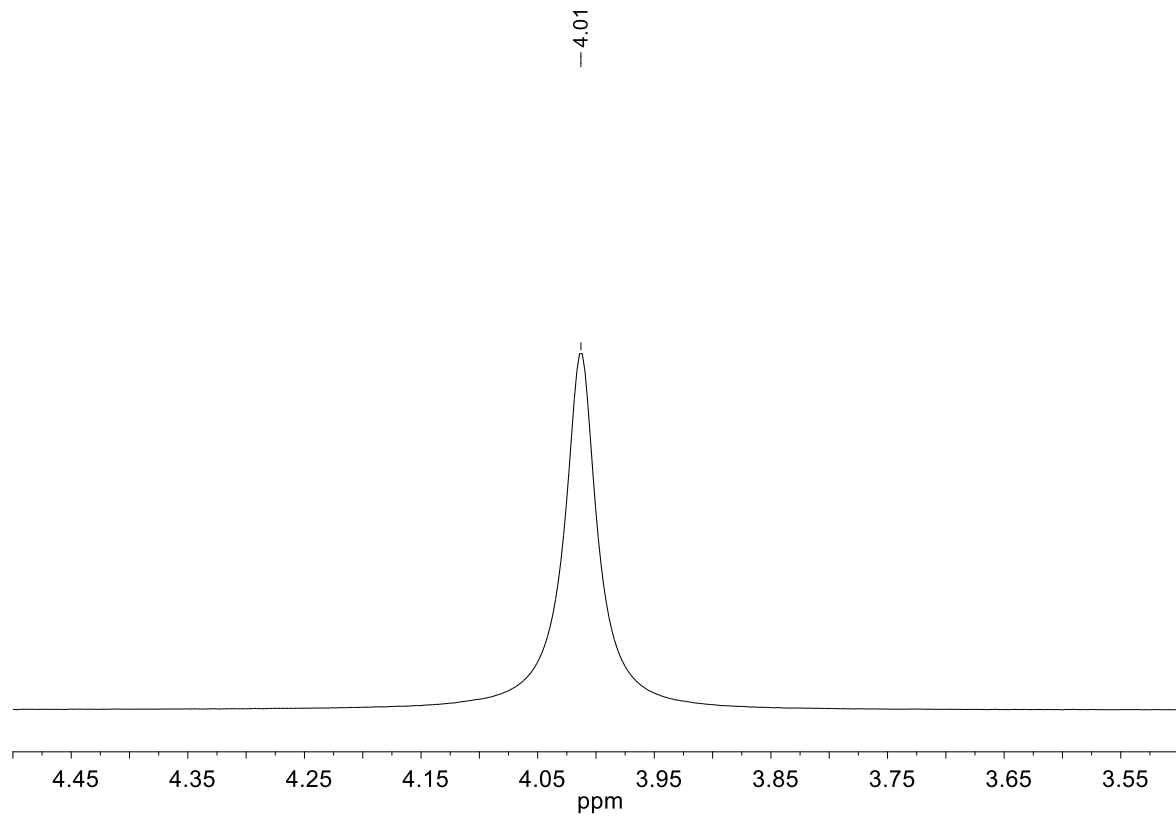


**Figure S21.** <sup>7</sup>Li NMR spectrum of **6**.

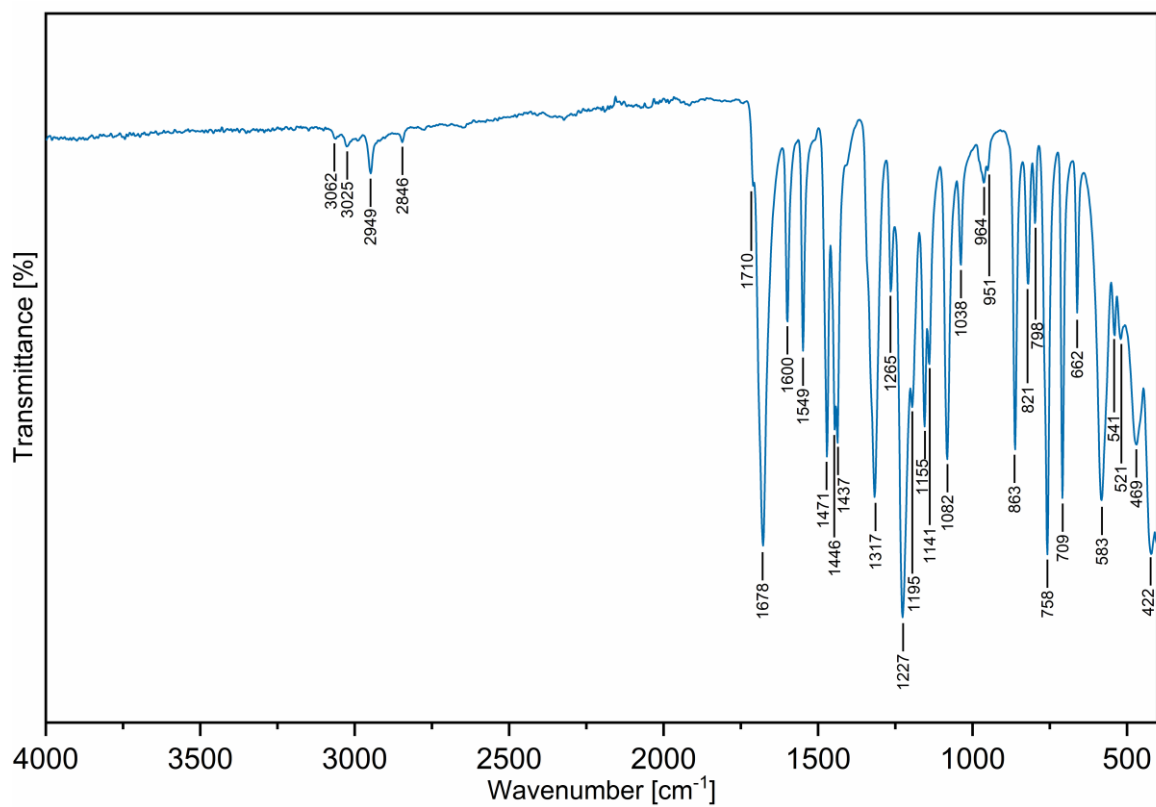


**Figure S22.** FTIR-ATR spectrum of **6**.

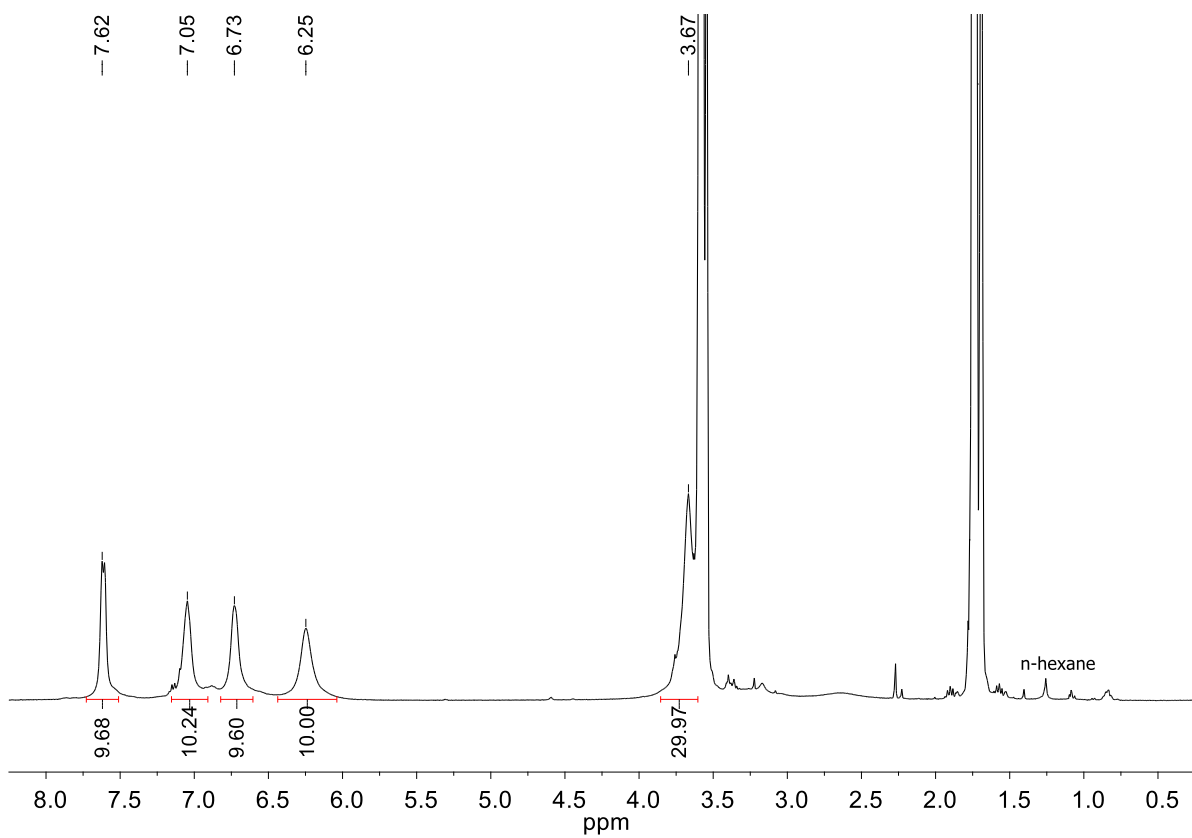


**Figure 23.**  $^1\text{H}$  NMR spectrum of **7** in  $\text{THF-d}_8$ .

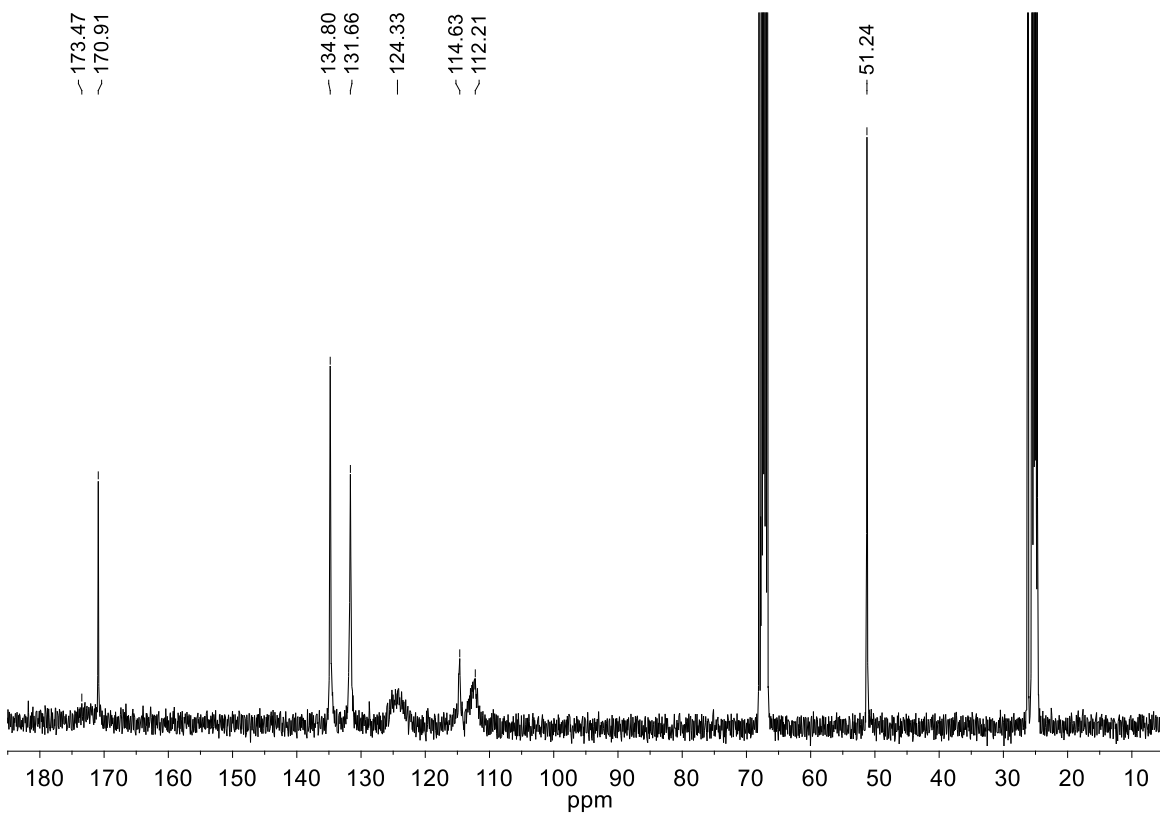


**Figure S24.**  $^{13}\text{C}$  NMR spectrum of **7** in  $\text{THF-d}_8$ .

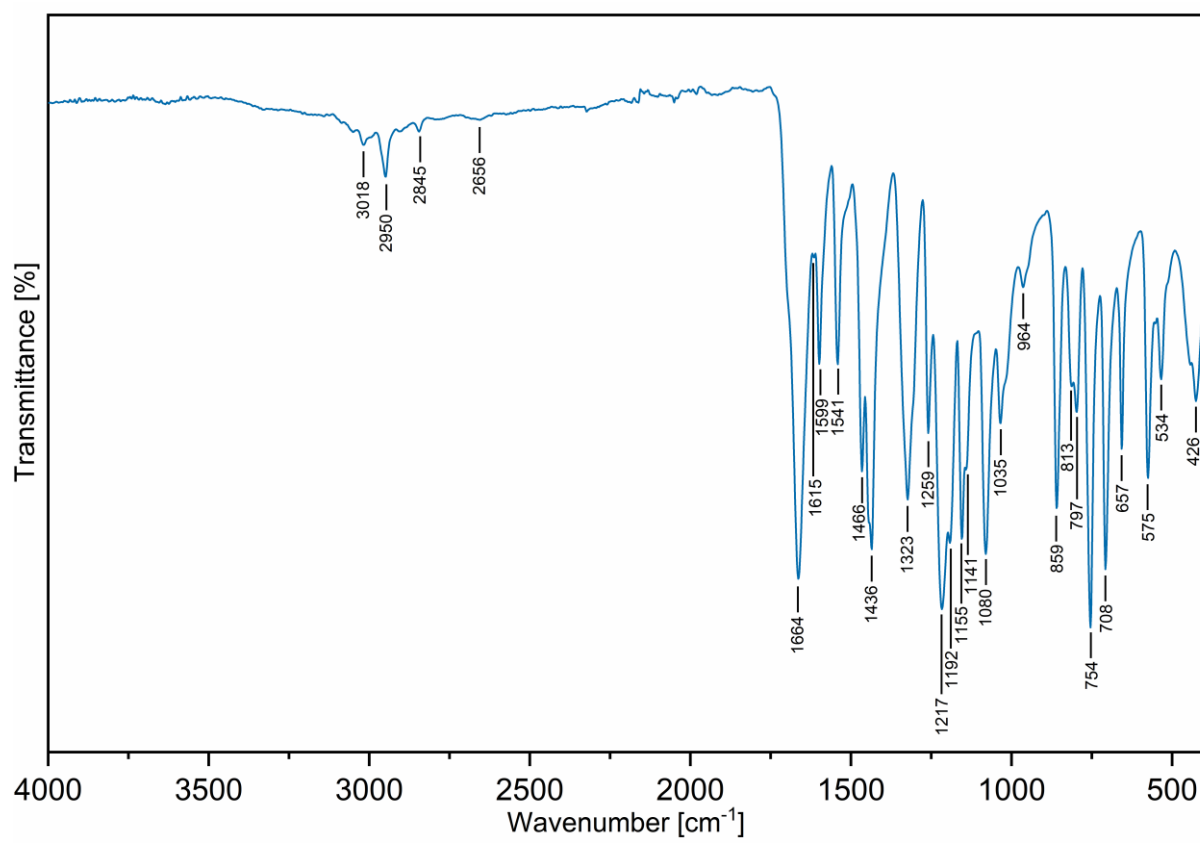


**Figure S25.** FTIR-ATR spectrum of **7**.

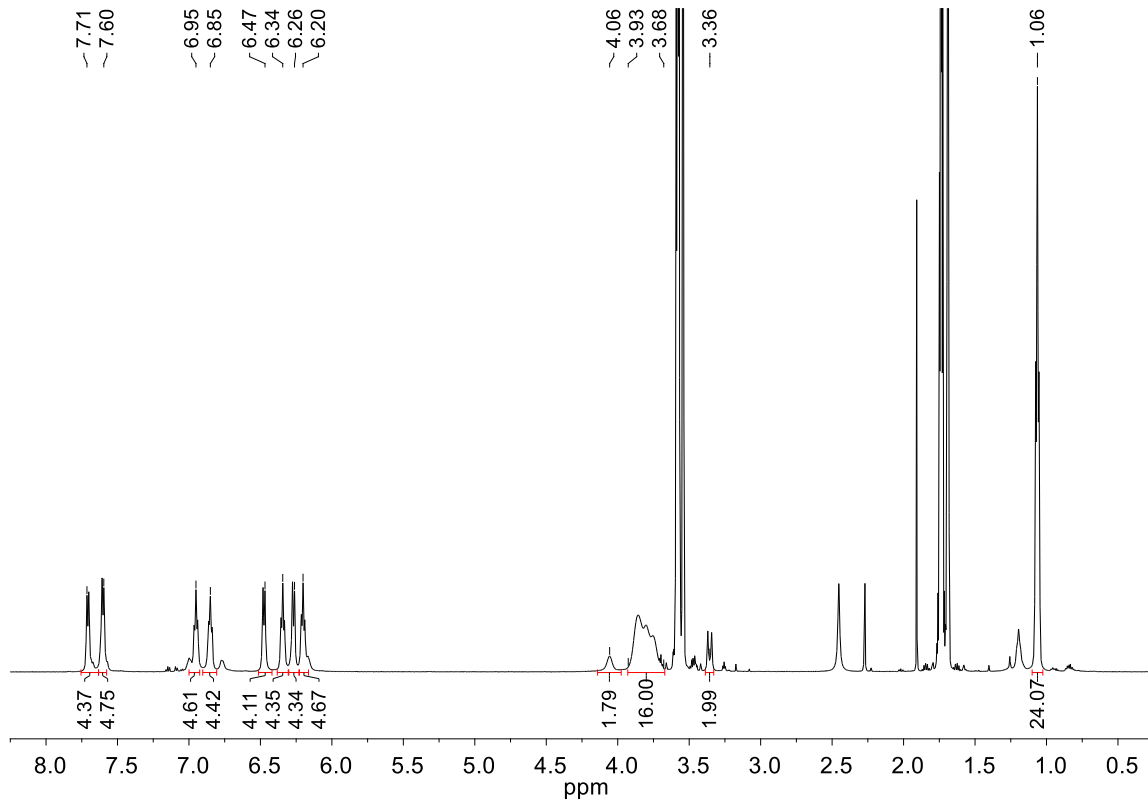


**Figure S26.**  $^1\text{H}$  NMR spectrum of **8** in  $\text{THF}-\text{d}_8$ .

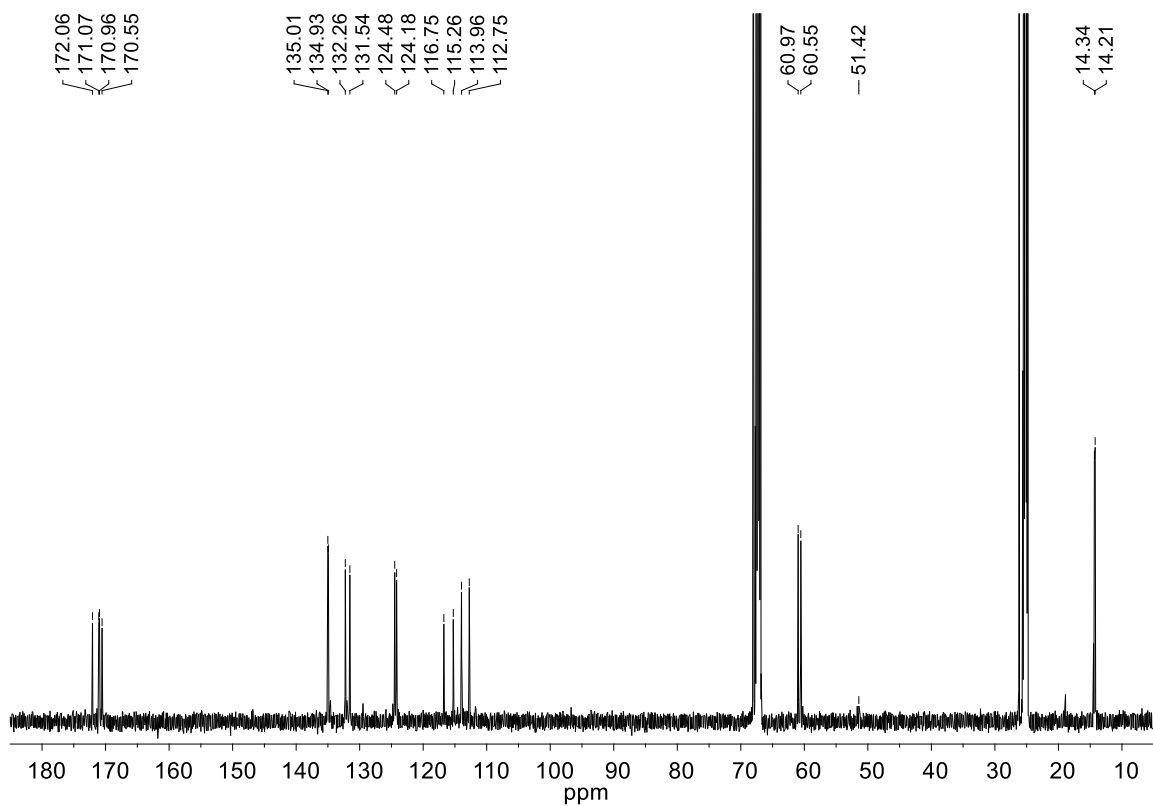


**Figure S27.**  $^{13}\text{C}$  NMR spectrum of **8** in THF-d<sub>8</sub>.

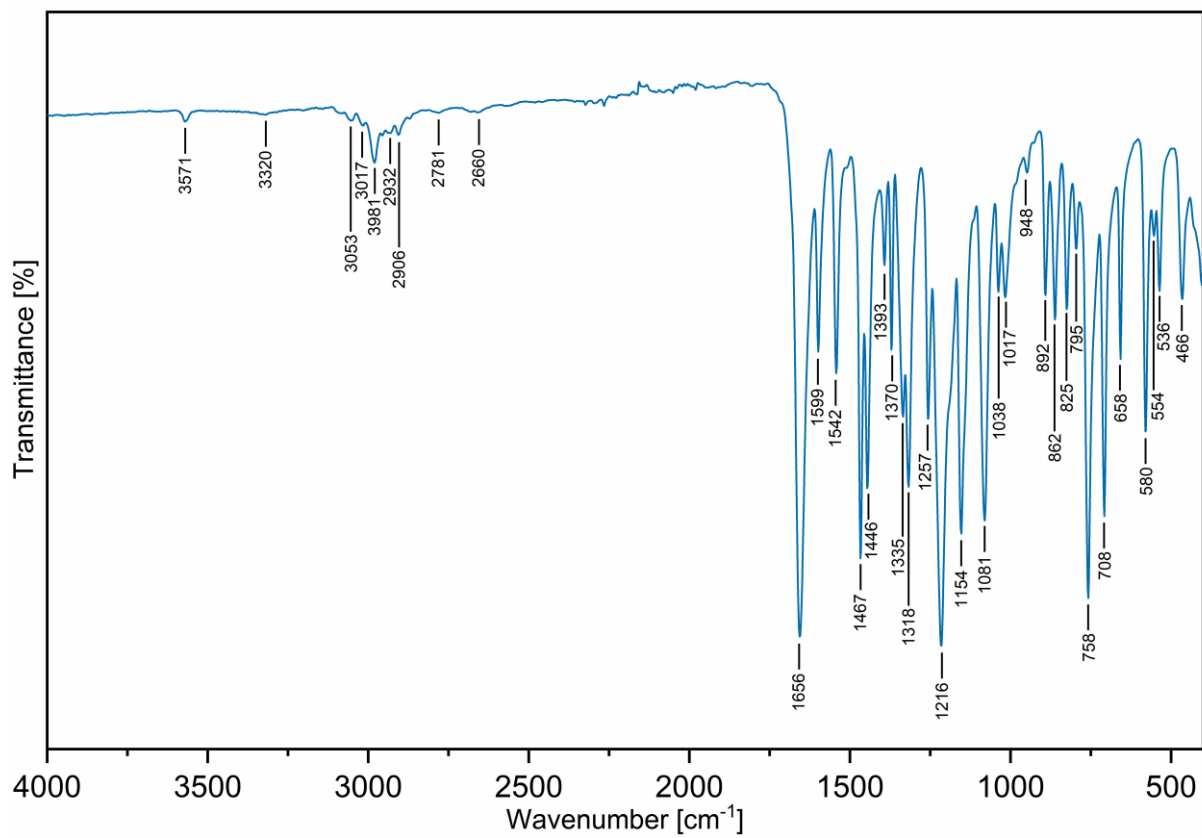


**Figure S28.** FTIR-ATR spectrum of **8**.

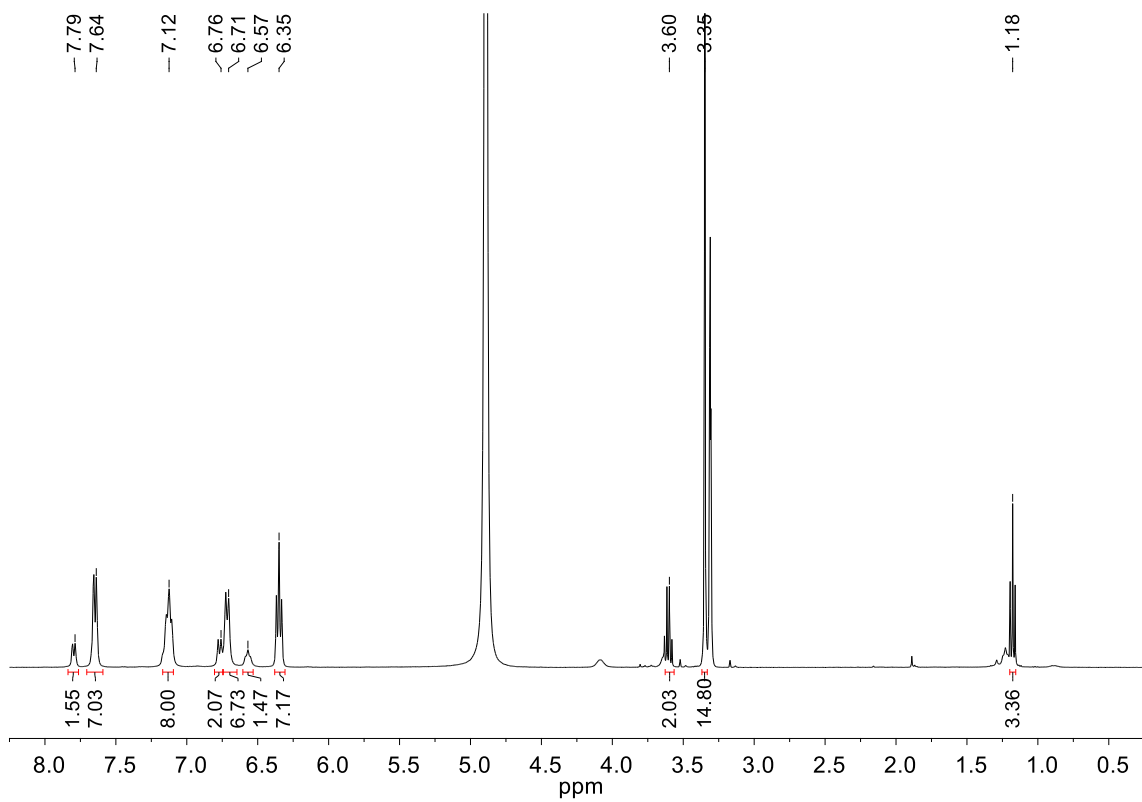


**Figure S29.** <sup>1</sup>H NMR spectrum of **9** in MeOH-d<sub>4</sub>.

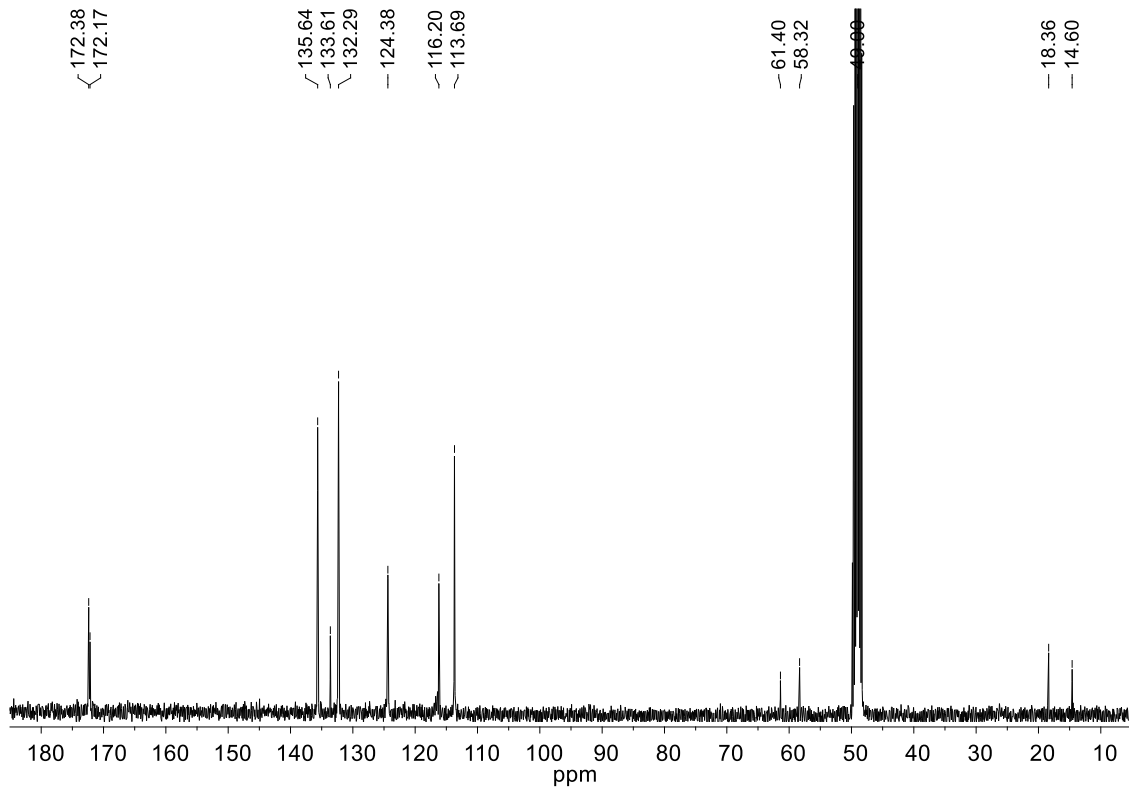


**Figure S30.** <sup>13</sup>C NMR spectrum of **9** in MeOH-d<sub>4</sub>.

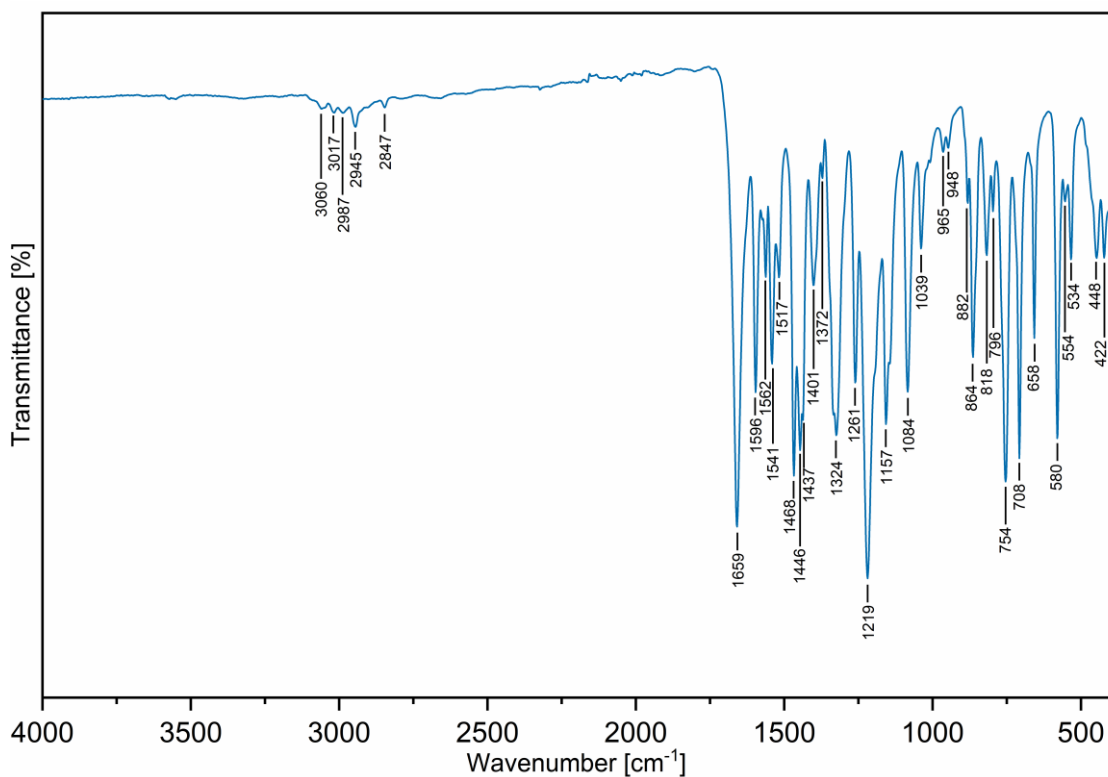


**Figure S31.** FTIR-ATR spectrum of **9**.

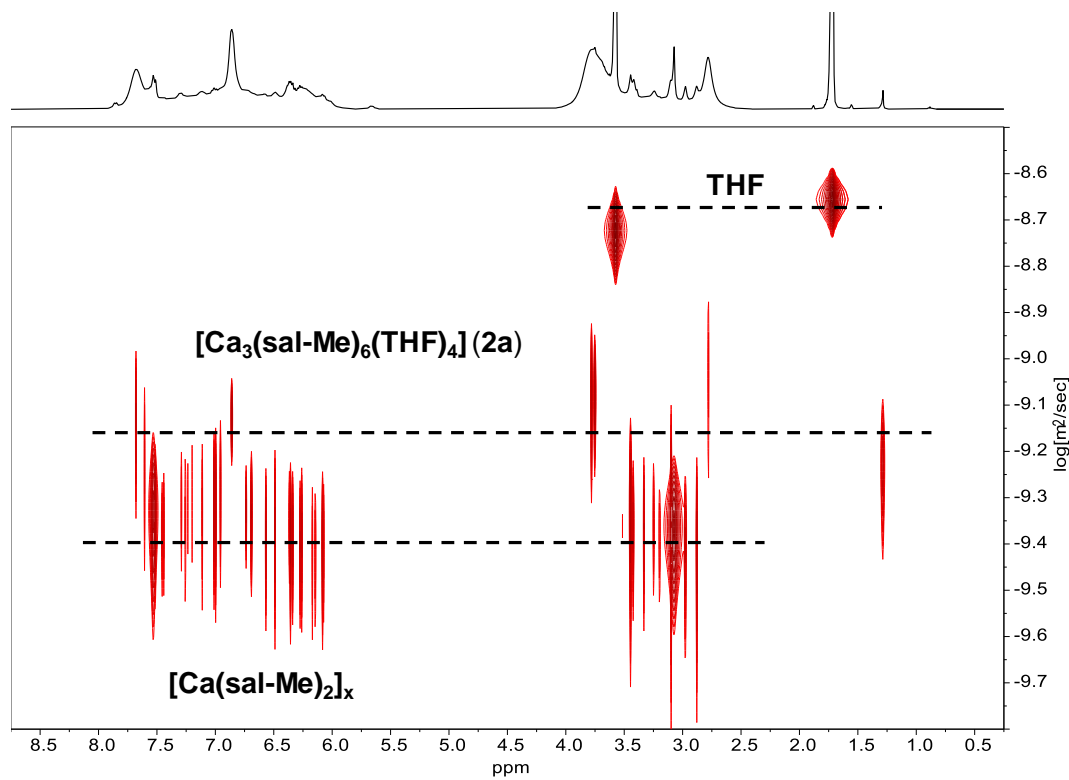


**Figure S32.**  $^1\text{H}$  DOSY NMR spectrum of **1** in  $\text{THF-d}_8$ .

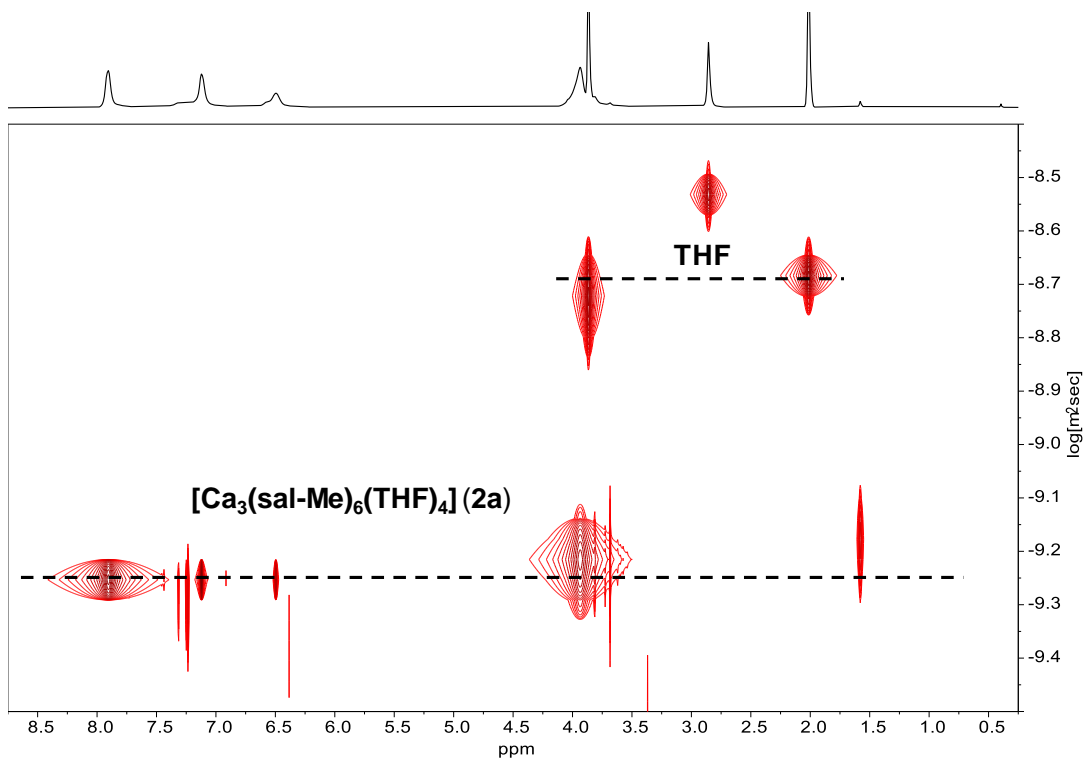


**Figure S33.**  $^1\text{H}$  DOSY NMR spectrum of **2** in  $\text{THF-d}_8$ .

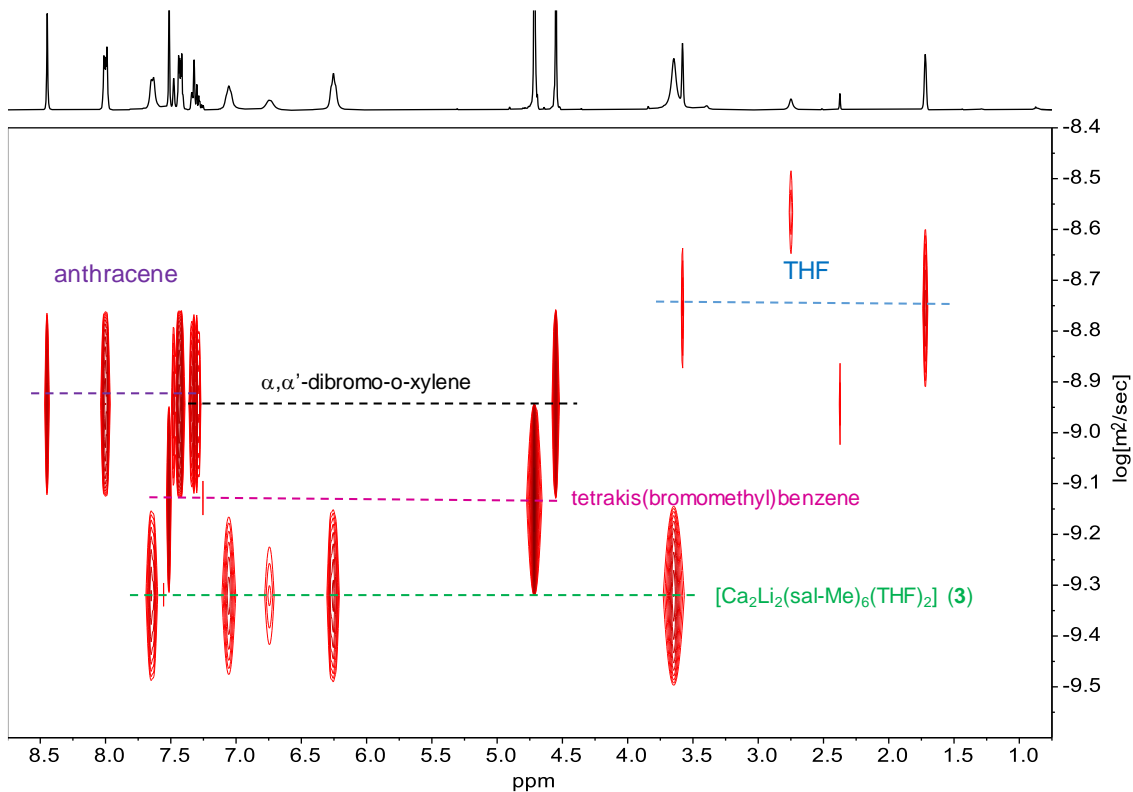


**Figure S34.**  $^1\text{H}$  DOSY NMR spectrum of a mixture of anthracene,  $\alpha,\alpha'$ -dibromo-o-xylene, 1,2,4,5-tetrakis(bromomethyl)benzene, and **3** in  $\text{THF-d}_8$ .

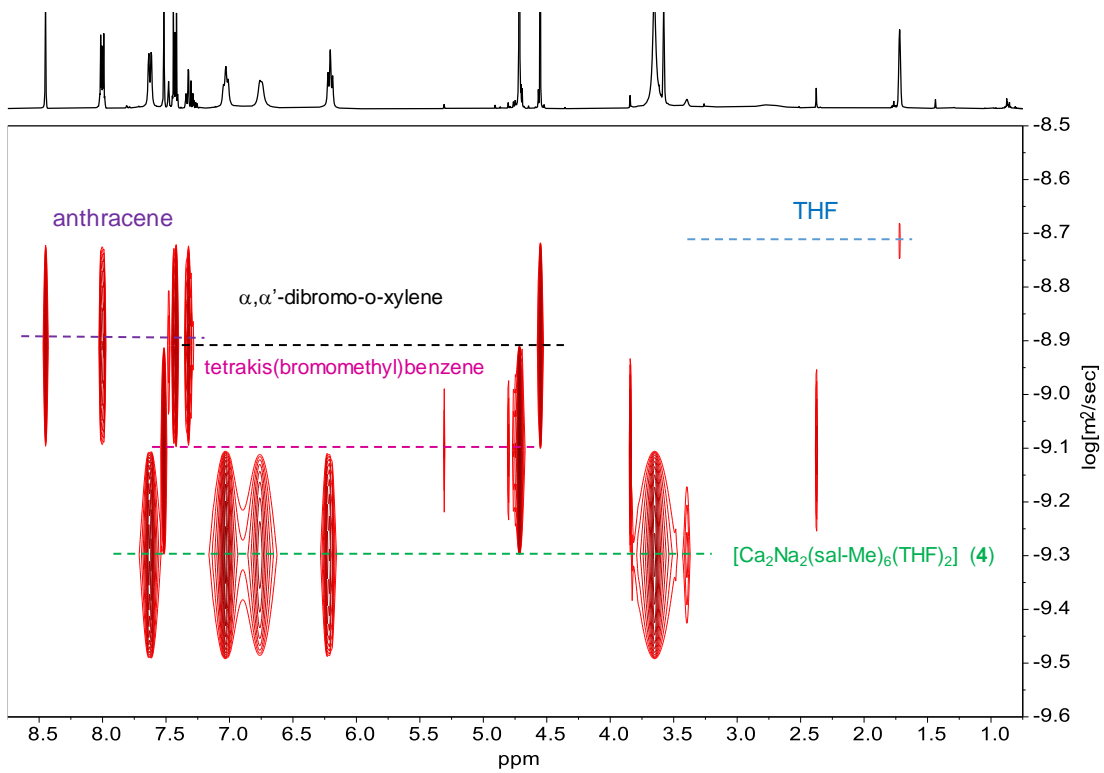


**Figure S35.**  $^1\text{H}$  DOSY NMR spectrum of a mixture of anthracene,  $\alpha,\alpha'$ -dibromo-o-xylene, 1,2,4,5-tetrakis(bromomethyl)benzene, and **4** in  $\text{THF-d}_8$ .

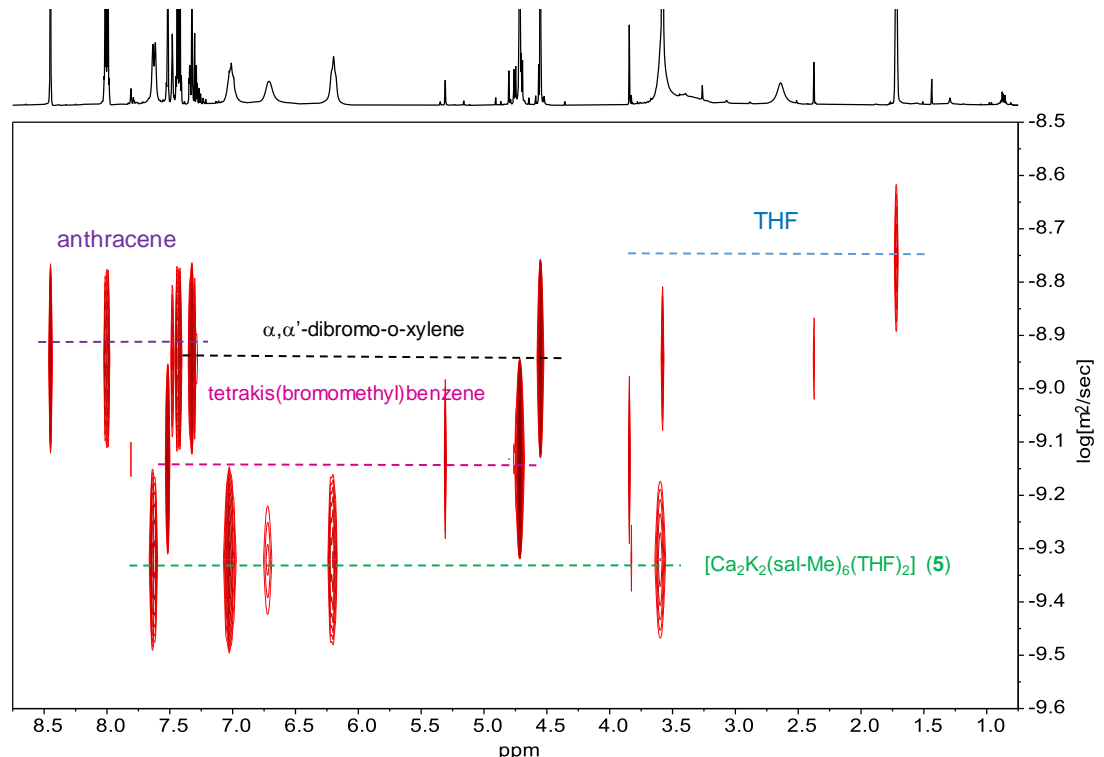


**Figure S36.**  $^1\text{H}$  DOSY NMR spectrum of a mixture of anthracene,  $\alpha,\alpha'$ -dibromo-o-xylene, 1,2,4,5-tetrakis(bromomethyl)benzene, and **5** in  $\text{THF-d}_8$ .

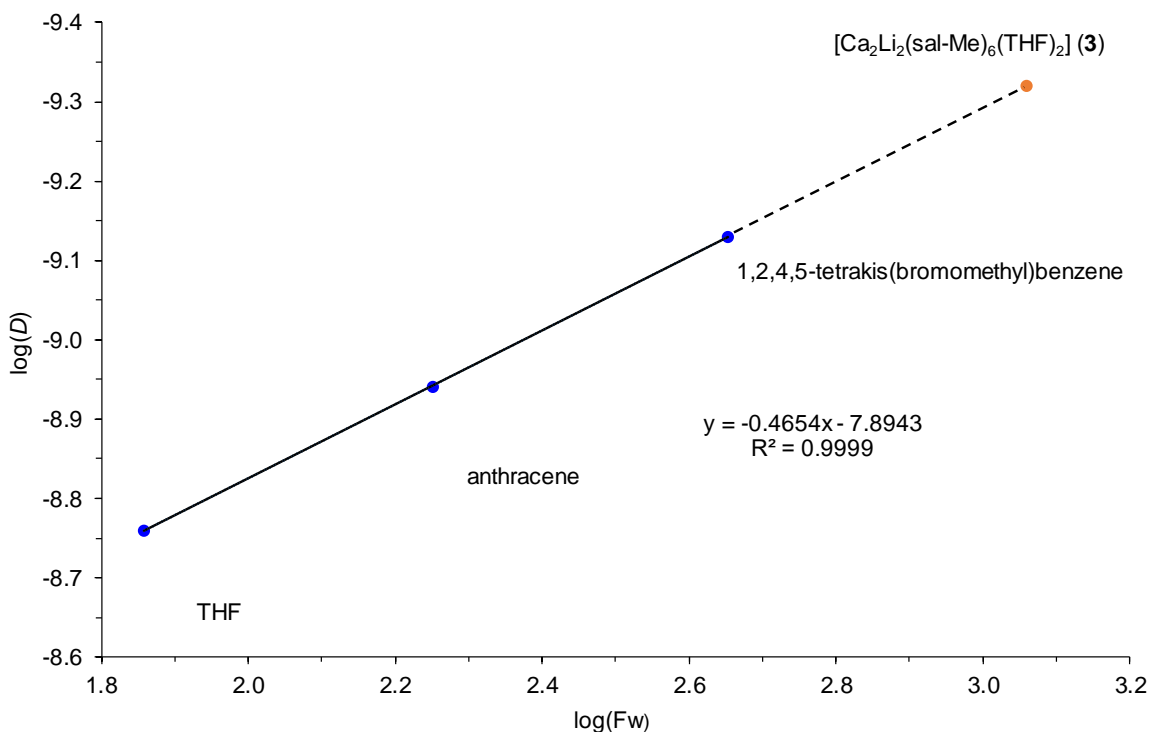


**Figure S37.** Plot of the diffusion coefficient ( $\log(D)$ ) versus formula weight ( $\log(F_w)$ ) for a mixture of anthracene, 1,2,4,5-tetrakis(bromomethyl)benzene, and **3** in THF-d<sub>8</sub>.

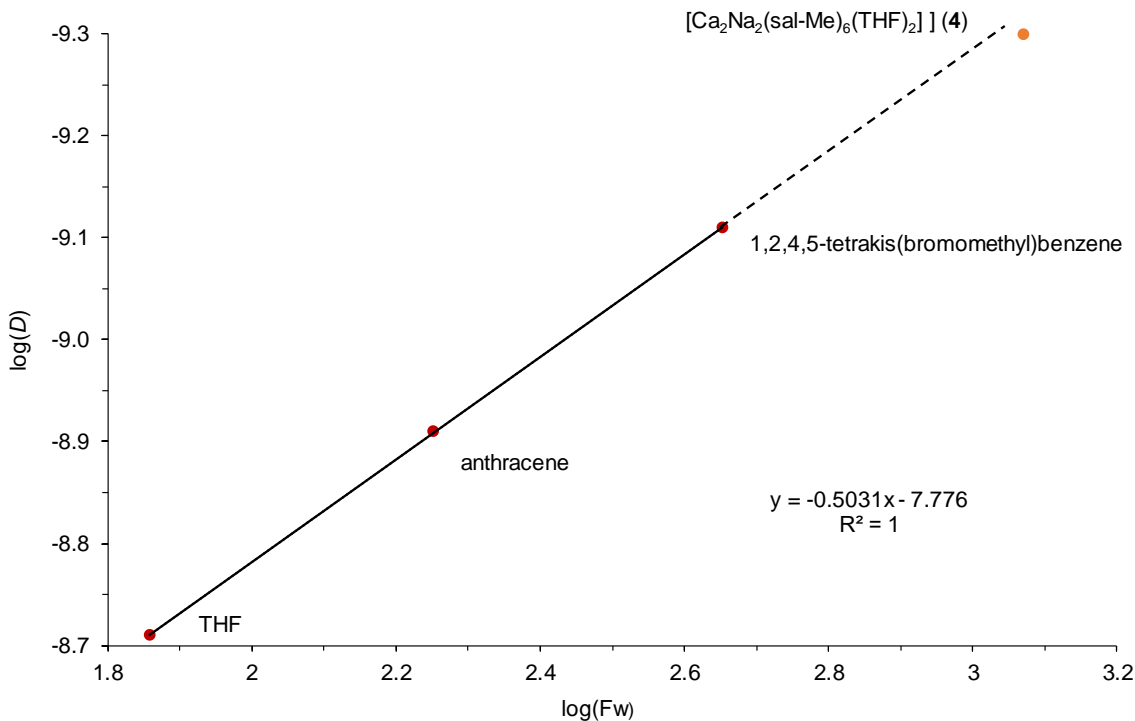


**Figure S38.** Plot of the diffusion coefficient ( $\log(D)$ ) versus formula weight ( $\log(F_w)$ ) for a mixture of anthracene, 1,2,4,5-tetrakis(bromomethyl)benzene, and **4** in THF-d<sub>8</sub>.

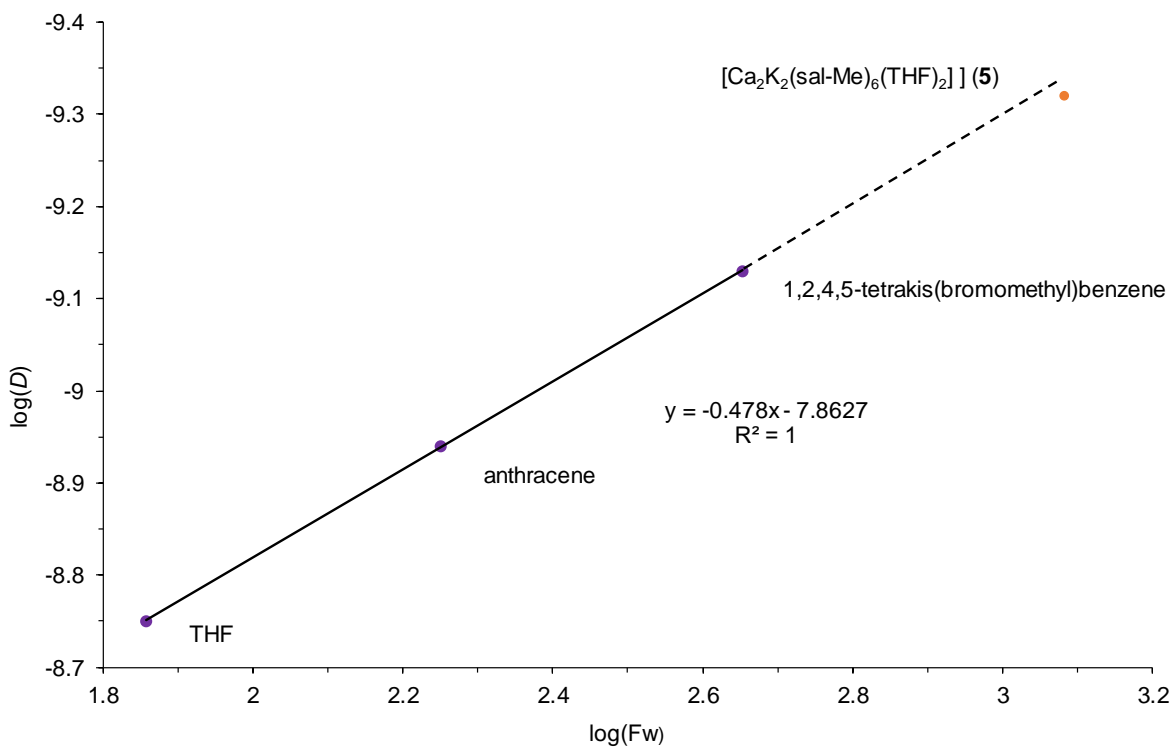


**Figure S39.** Plot of the diffusion coefficient ( $\log(D)$ ) versus formula weight ( $\log(F_w)$ ) for a mixture of anthracene, 1,2,4,5-tetrakis(bromomethyl)benzene, and **5** in THF-d<sub>8</sub>.

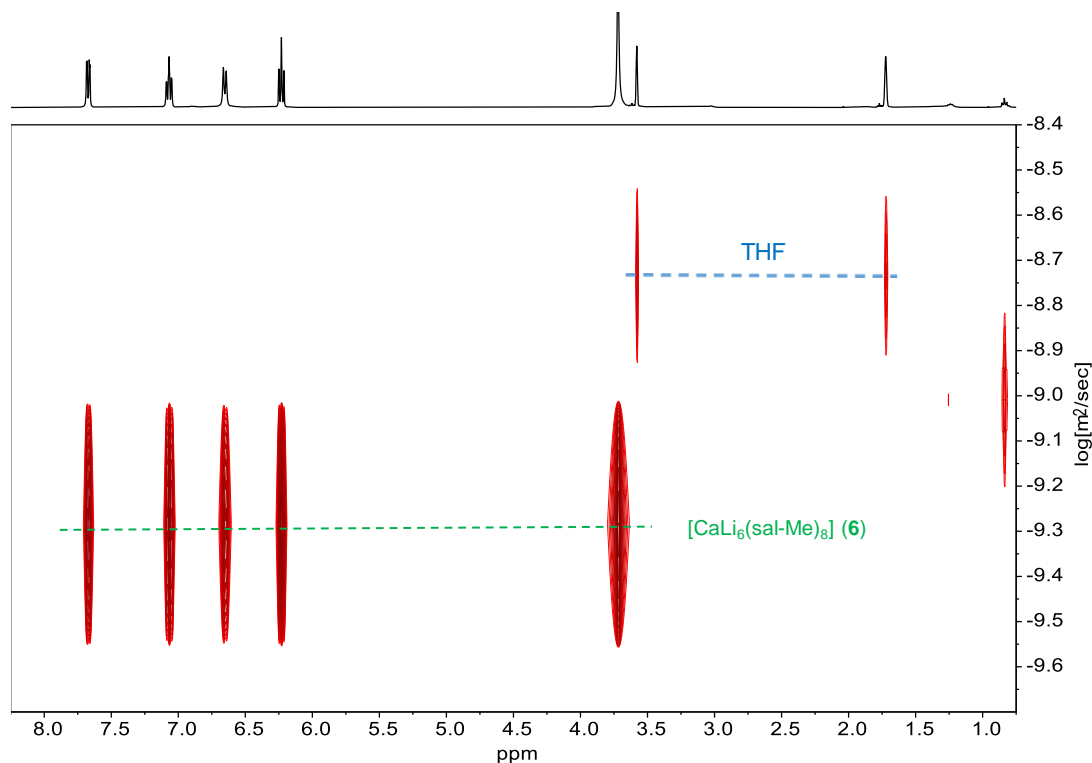


**Figure S40.**  $^1\text{H}$  DOSY NMR spectrum of **6** in THF-d<sub>8</sub>.

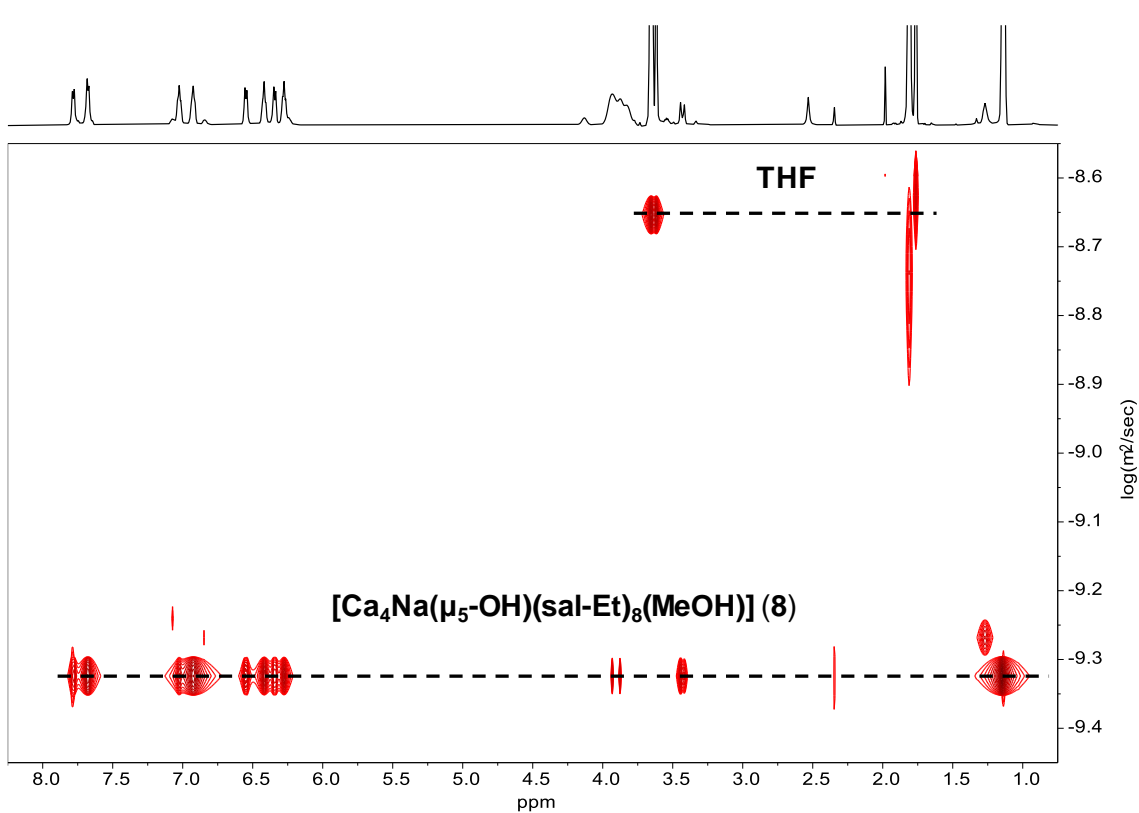
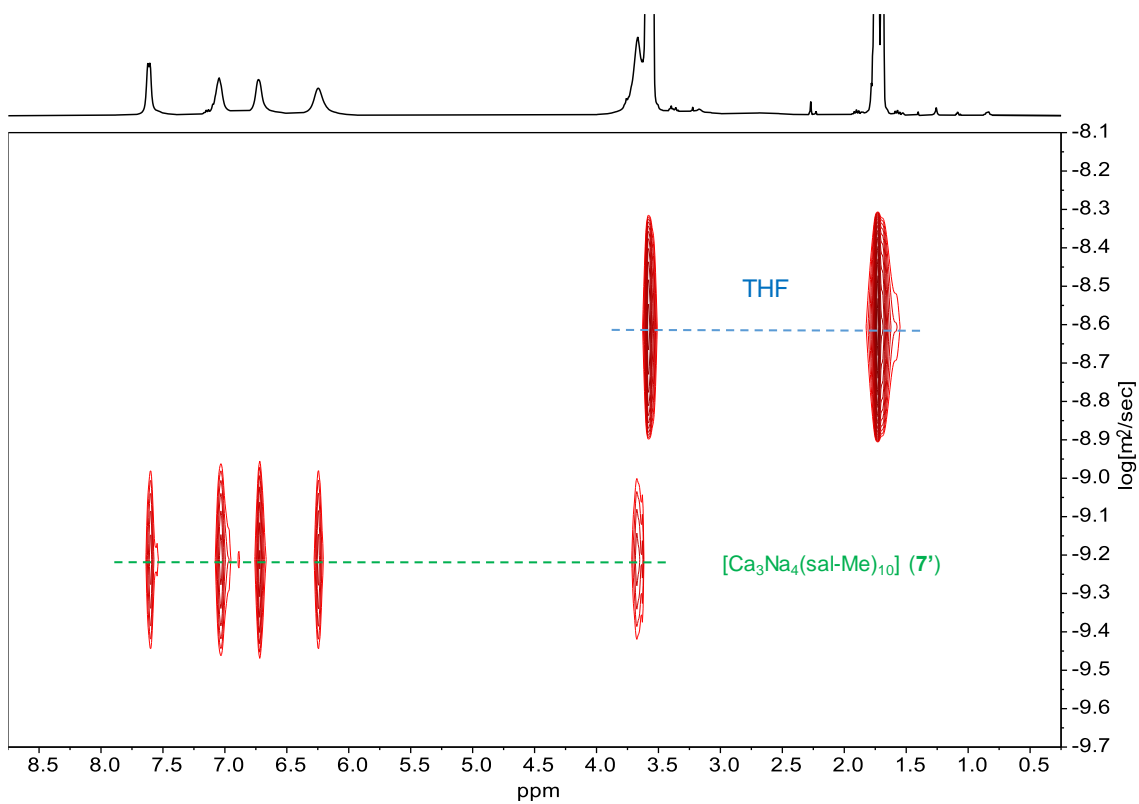


**Table S3.** Formula weights (FWs) and the hydrodynamic radii ( $r_H$ ) of **3-8** estimated from Stokes-Einstein Gierer-Wirtz method.

compound	$\log(D_x)$	$\log(D_{x,\text{norm}})$	T (°C)	FW (g/mol)	FW <sub>calc</sub> (g/mol)	$r_{\text{x-ray}}$ (Å)	$r_H$ (Å)
<b>1</b>	-9.1656	-9.135	22.2	$(342.35)_n$	920	-	8.35
	-9.399	-9.368			2752		12.03
<b>2 (2a)</b>	-9.252	-9.221	22.2	1315.49	1230	8.71	9.19
<b>3</b>	-9.320	-9.194	22.5	1145.09	1074	7.76	8.79
<b>4</b>	-9.300	-9.224	22.9	1177.18	1275	7.85	9.31
<b>5</b>	-9.320	-9.204	23.2	1209.40	1158	-	9.02
<b>6</b>	-9.280	-9.184	24.0	1290.84	1069		8.78
<b>7</b>	-9.230	-9.254	21.9	1723.59	1448	9.32	9.71
<b>8</b>	-9.324	-9.304	21.9	1553.68	1904	8.22	10.64

**Table S4.** Diffusion coefficients and formula weight for **3-5** determined using calibration plots.

compound	$\log(D_x)$	FW (g/mol)	FW <sub>calc</sub> (g/mol)
<b>3</b>	-9.320	1145.09	1157
<b>4</b>	-9.300	1177.18	1070
<b>5</b>	-9.320	1209.40	1119

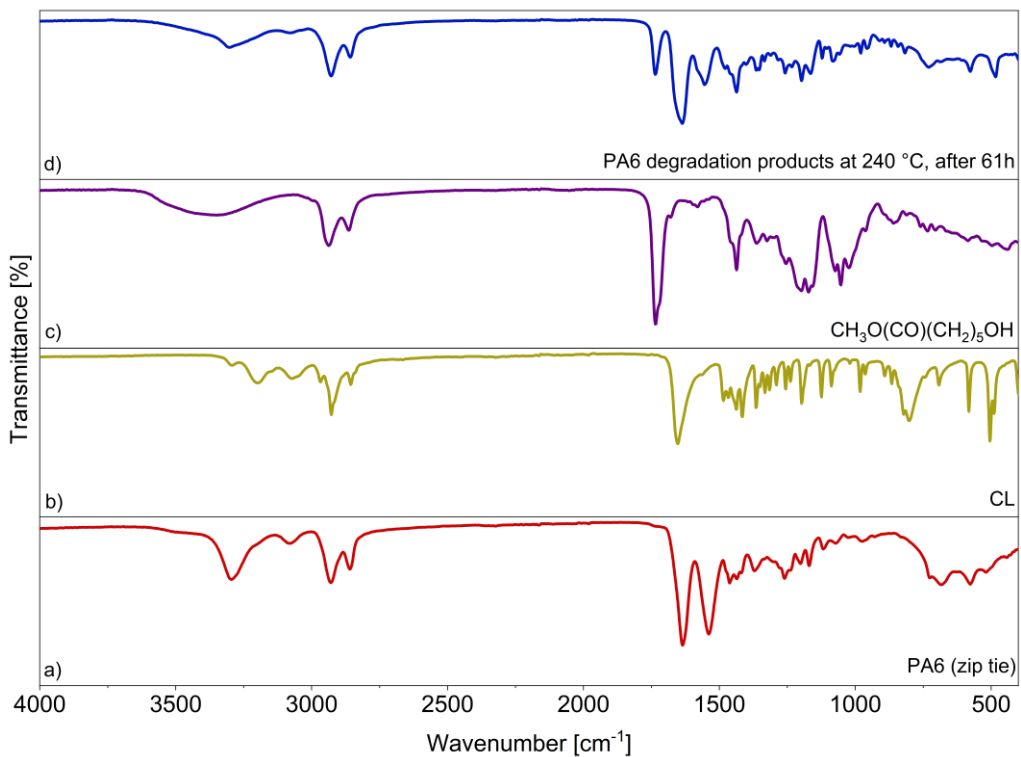


**Figure S43.** The comparison of FTIR-ATR spectra of PA6 (a), CL (b),  $\text{CH}_3\text{O}(\text{CO})(\text{CH}_2)_5\text{OH}$  (c), and PA6 degradation products at 240°C (d).

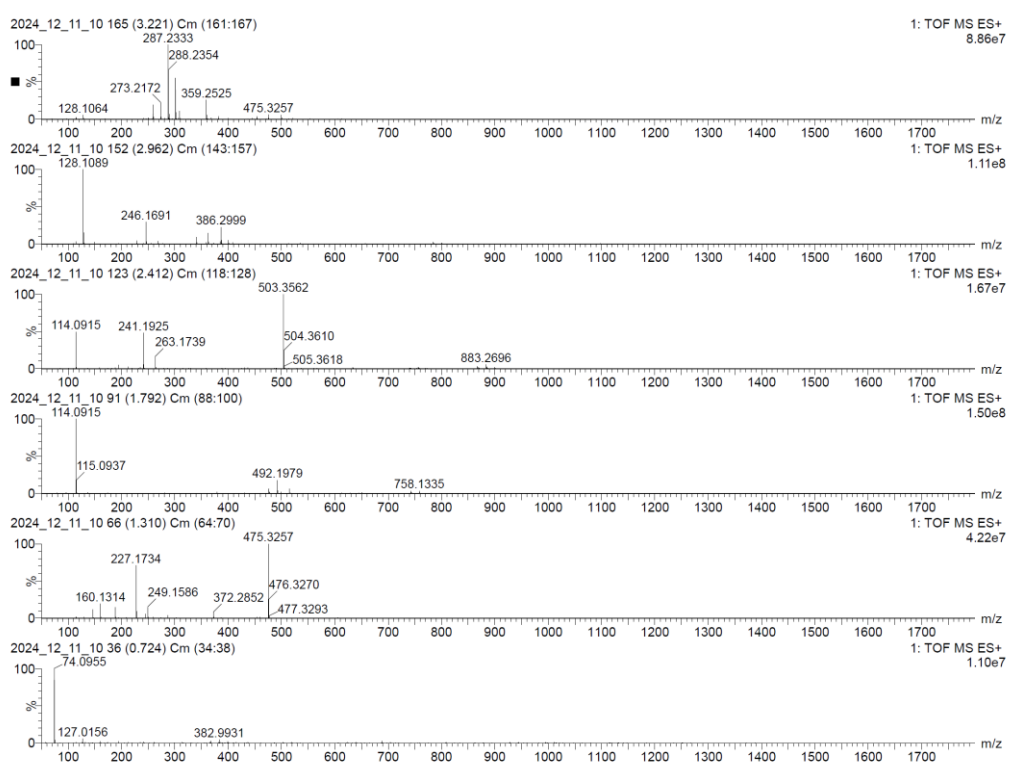


**Figure S44.** ESI-MS spectra of organic products obtained from PA6 methanolysis using **2** as catalyst after 61 h at 240 °C, recorded after 43, 78, 107, 144, 177, and 193 seconds.

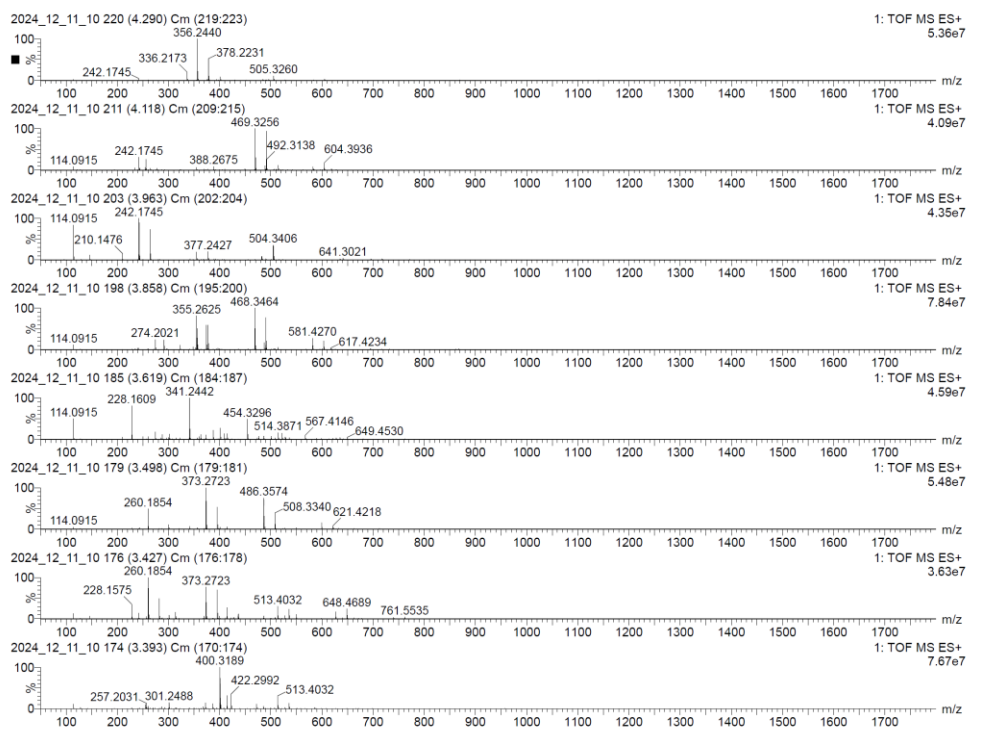


**Figure S45.** ESI-MS spectra of organic products obtained from PA6 methanolysis using **2** as catalyst after 61 h at 240 °C, recorded after 203, 205, 209, 217, 231, 237, 247, and 257 seconds.

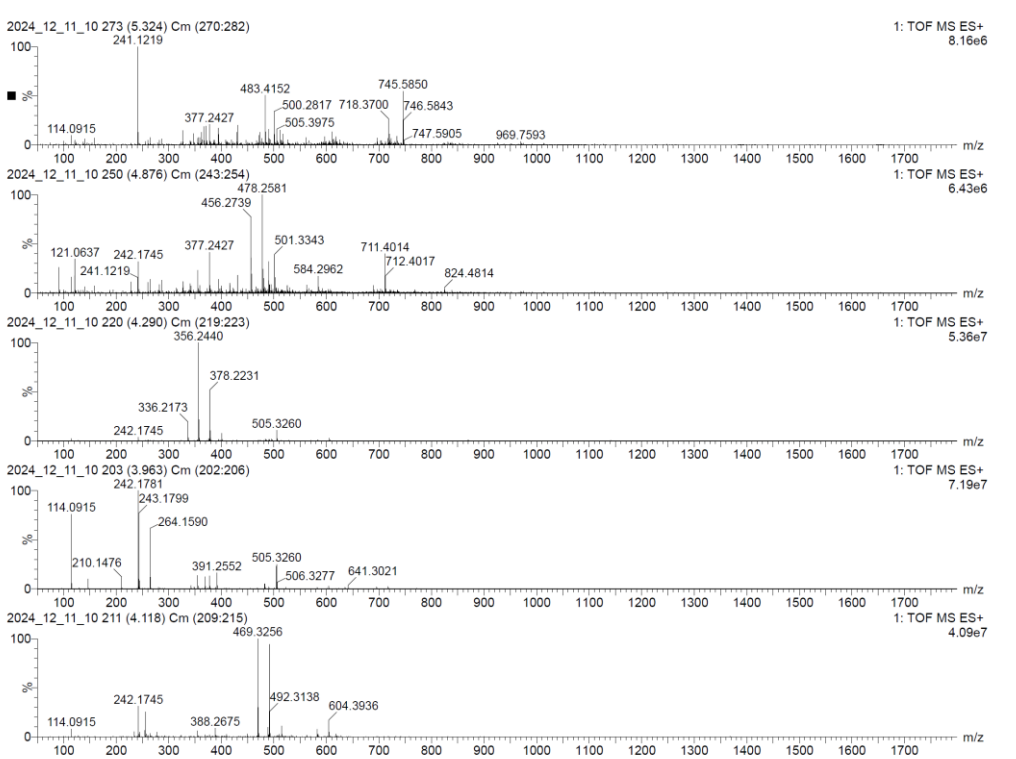


**Figure S46.** ESI-MS spectra of organic products obtained from PA6 methanolysis using **2** as catalyst after 61 h at 240 °C, recorded after 292, and 319 seconds.

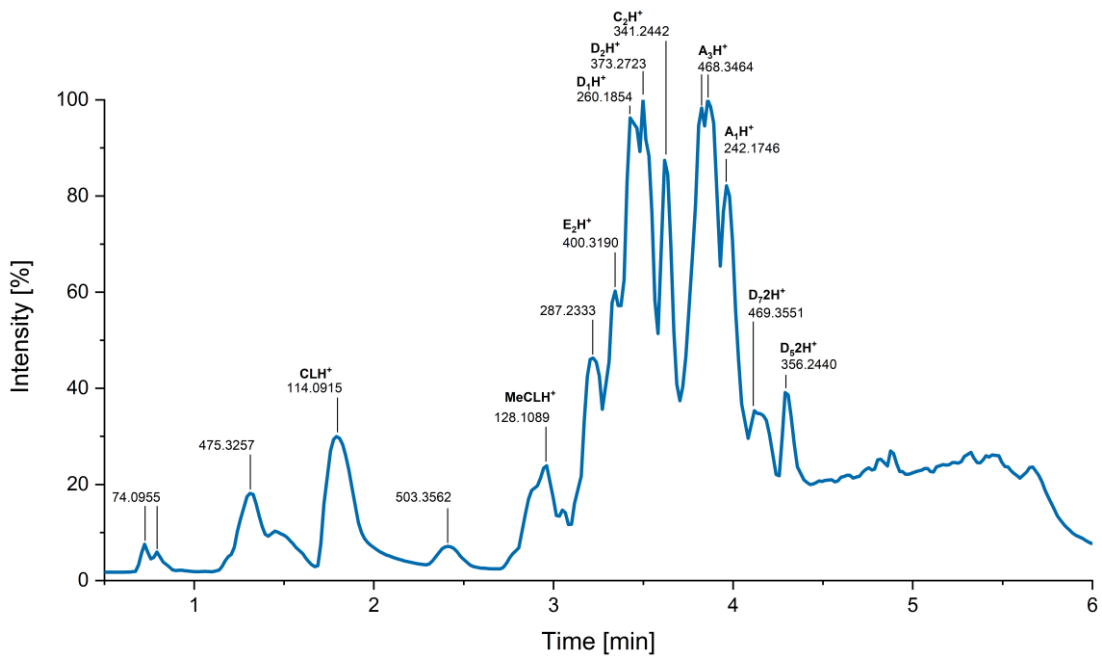


**Figure S47.** LC-MS chromatogram of organic products obtained from PA6 methanolysis using **2** as catalyst after 61 h at 240 °C.

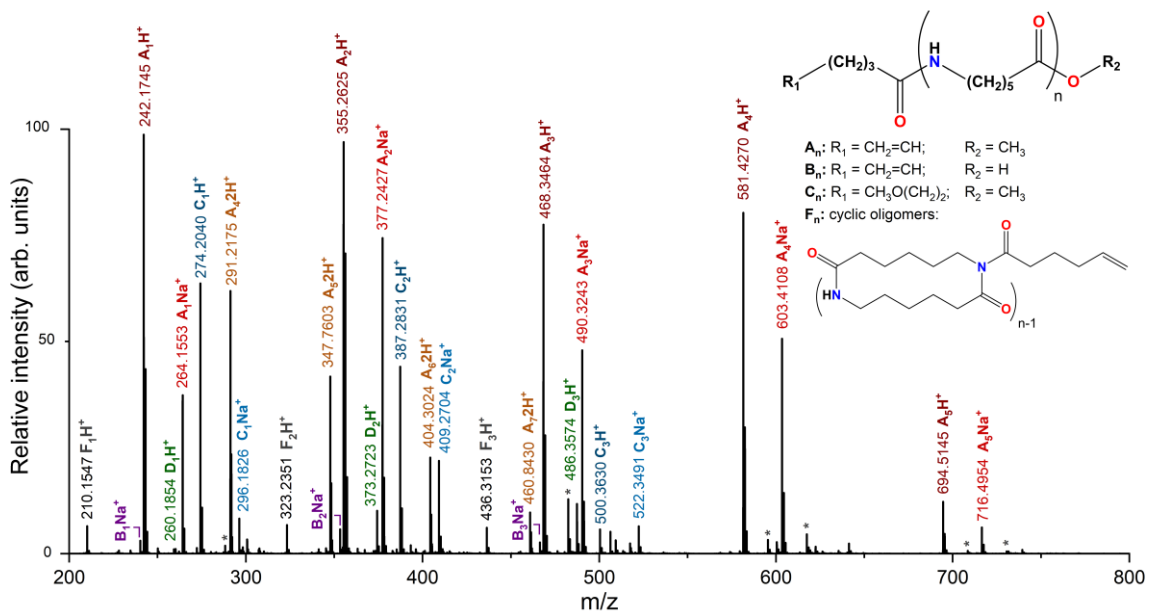


**Figure S48.** ESI-MS spectrum of organic products obtained from PA6 methanolysis using **2** as catalyst after 61 h at 240 °C, recorded after 231 seconds.

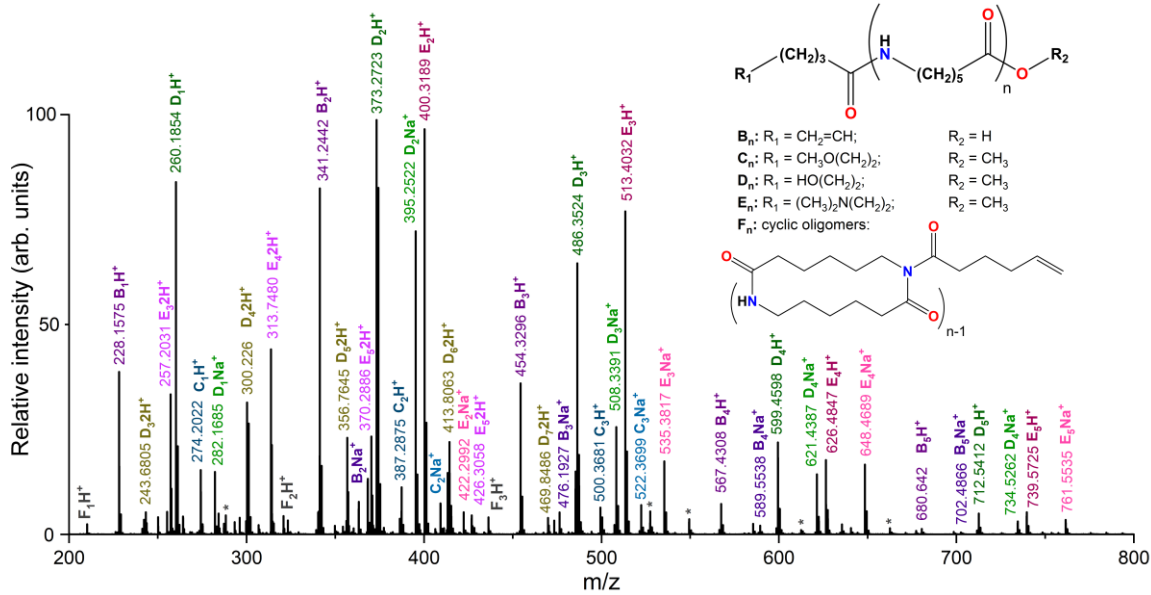


**Figure S49.** ESI-MS spectrum of organic products obtained from PA6 methanolysis using **2** as catalyst after 61 h at 240 °C, recorded after 209 seconds.

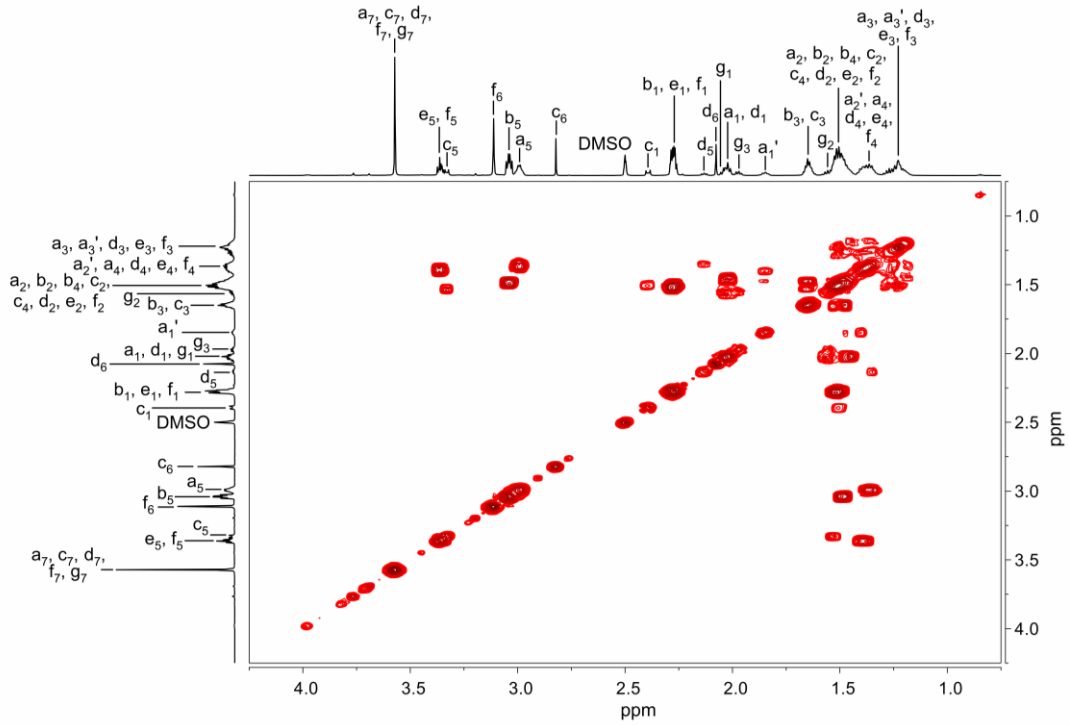


**Figure S50.**  $^1\text{H} - ^1\text{H}$  COSY NMR spectrum in DMSO-d<sub>6</sub> of organic products obtained from PA6 methanolysis using **2** as catalyst after 61 h at 240 °C.

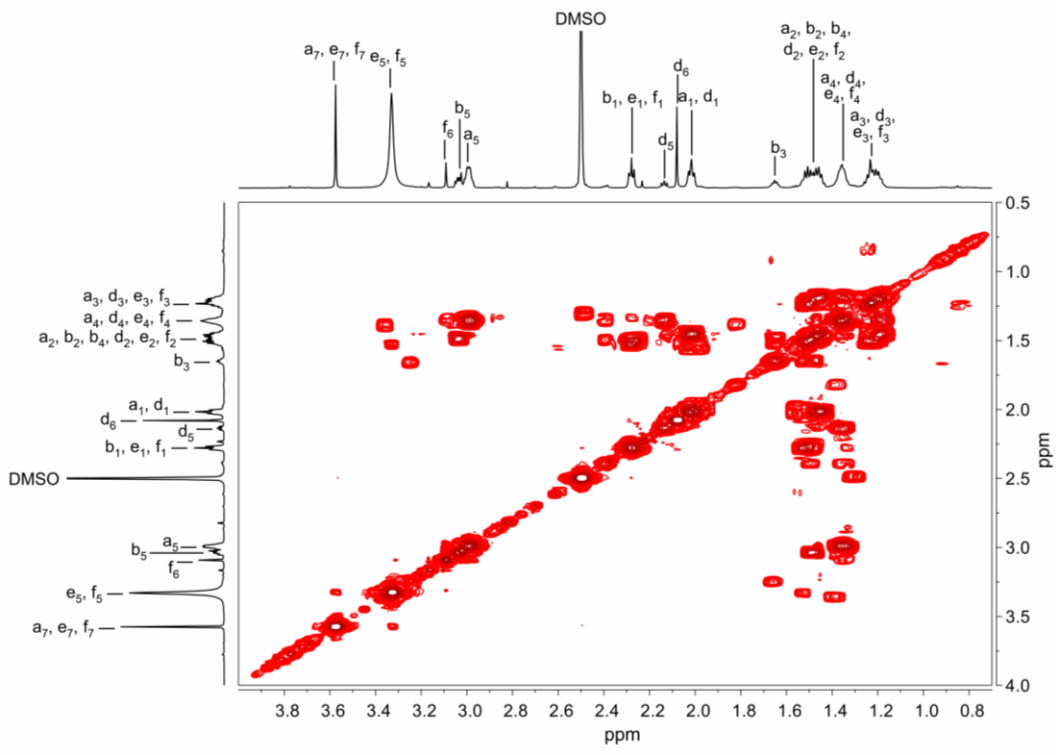


**Figure S51.**  $^1\text{H}$  -  $^1\text{H}$  COSY NMR spectrum in  $\text{DMSO-d}_6$  of organic products obtained from PA6 methanolysis using **2** as catalyst after 8 h at 220 °C.

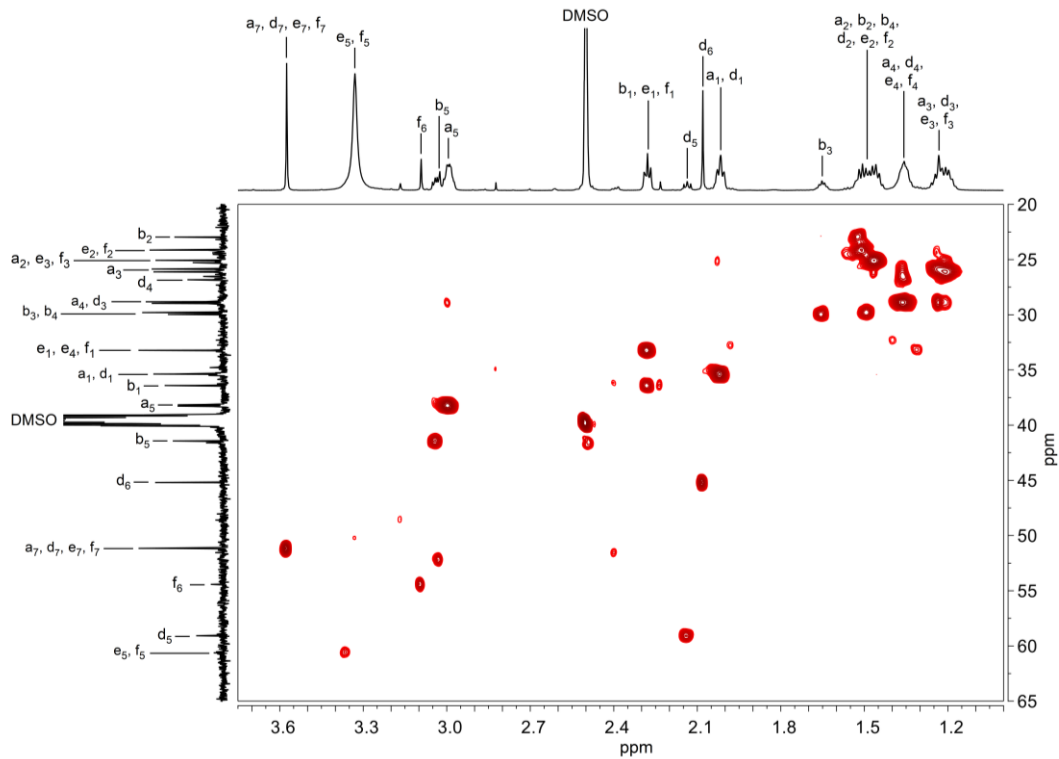


**Figure S52.**  $^1\text{H}$  –  $^{13}\text{C}$  HSQC NMR spectrum in  $\text{DMSO-d}_6$  of organic products obtained from PA6 methanolysis using **2** as catalyst after 8 h at 220 °C.

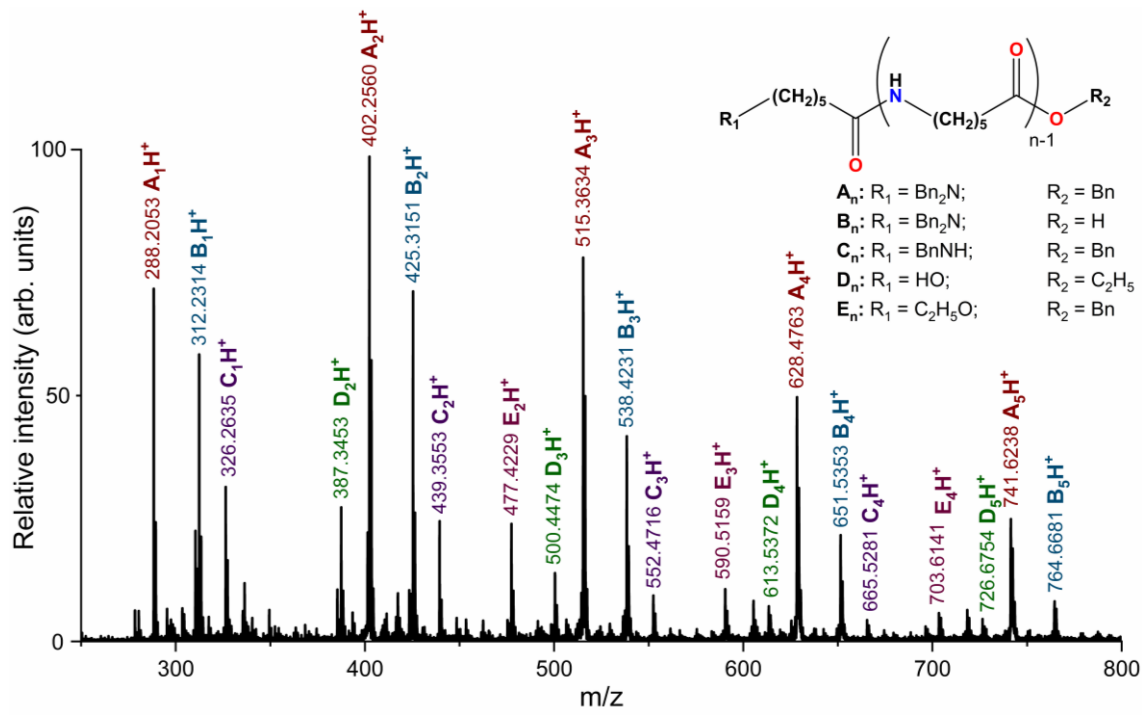


**Figure S53.** ESI-MS spectrum of liquid organic products obtained from PA6 alcoholytic reaction using BnOH and **13** as catalyst after 25 h at 220 °C.

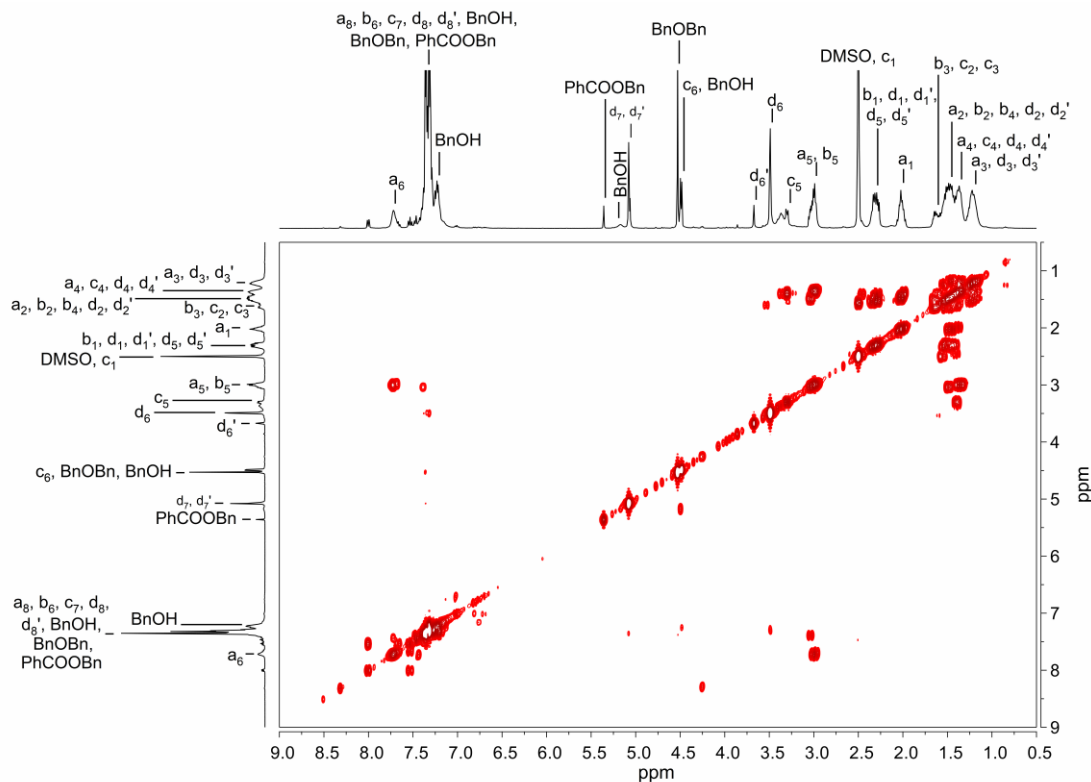


**Figure S54.** <sup>1</sup>H - <sup>1</sup>H COSY NMR spectrum in DMSO-d<sub>6</sub> of liquid organic products obtained from PA6 alcoholytic reaction using BnOH and **13** as catalyst after 25 h at 220 °C.

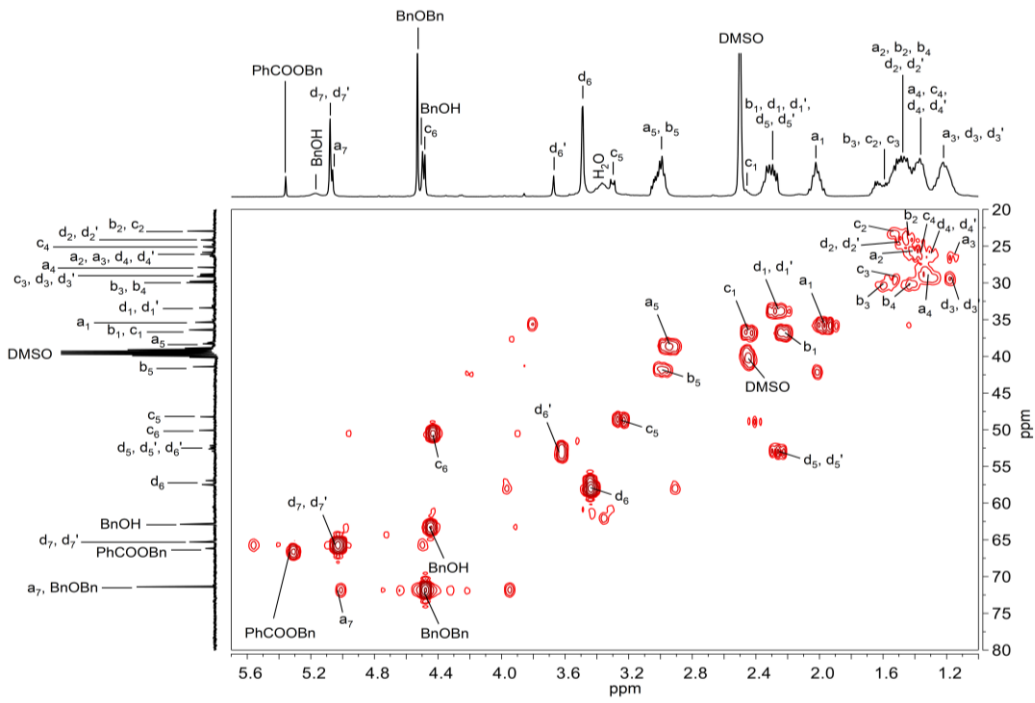


**Figure S55.**  $^1\text{H} - ^{13}\text{C}$  HMQC NMR spectrum in  $\text{DMSO-d}_6$  of liquid organic products obtained from PA6 alcoholysis using  $\text{BnOH}$  and **13** as catalyst after 25 h at  $220^\circ\text{C}$ .

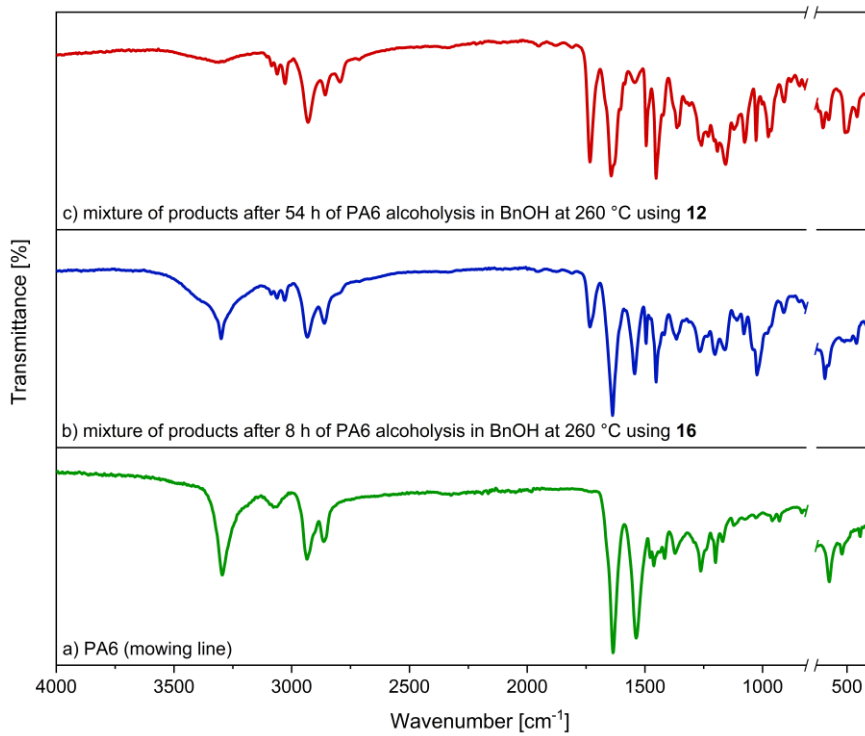


**Figure S56.** Comparison of FTIR-ATR spectra of PA6 (a), the product mixture from PA6 alcoholysis using benzyl alcohol and **16** after 8 h at  $260^\circ\text{C}$  (b), and the product mixture from PA6 alcoholysis using benzyl alcohol and **12** after 54 h at  $260^\circ\text{C}$ . The spectral region around  $750\text{ cm}^{-1}$  was removed due to intense signals from benzyl alcohol.

**Table S5.** Summary of alcoholysis of PA6, using methanol in the presence of **2-21** at 200-240 °C after 8h.<sup>a</sup>

No.	Catalyst	T [°C]	C [%]	I [%]	II [%]	III [%]	IV [%]	V [%]	VI [%]	VII [%]
1	catalyst free	240	60	31	10	1	5	9	3	1
2		220	26	16	4	<1	1	4	1	<1
3		200	14	6	5	<1	<1	3	<1	0
4	$[\text{Ca}_3(\text{sal-Me})_6(\text{MeOH})_2]$ ( <b>2</b> )	240	71	34	12	1	7	12	4	1
5		220	34	20	6	<1	2	4	2	<1
6		200	5	3	2	0	<1	<1	<1	0
7	$[\text{Ca}_2\text{Li}_2(\text{sal-Me})_6(\text{THF})_2]$ ( <b>3</b> )	240	92	38	20	2	10	14	5	3
8		220	60	30	12	1	4	10	2	1
9		200	15	7	4	<1	<1	3	1	0
10	$[\text{Ca}_2\text{Na}_2(\text{sal-Me})_6(\text{MeOH})_4]$ ( <b>4</b> )	240	89	39	16	1	8	14	8	3
11		220	48	25	9	<1	3	8	2	1
12		200	22	11	6	<1	1	3	1	0
13	$[\text{Ca}_2\text{K}_2(\text{sal-Me})_6(\text{MeOH})_4]$ ( <b>5</b> )	240	81	38	14	1	8	12	6	2
14		220	33	18	6	<1	2	5	2	<1
15		200	15	9	4	<1	<1	1	1	<1
16	$[\text{CaLi}_6(\text{sal-Me})_8]$ ( <b>6</b> )	240	93	35	24	3	9	12	7	3
17		220	84	35	20	2	8	11	7	1
18		200	61	29	14	1	3	12	2	<1
19	$[\text{Ca}_3\text{Na}_4(\text{sal-Et})_{10}(\text{Hsal-Et})_2]$ ( <b>7</b> )	240	93	40	20	2	9	12	7	3
20		220	38	18	8	2	2	5	3	<1
11		200	8	4	2	0	<1	1	1	0
22	$[\text{Ca}_4\text{Na}(\mu_5\text{-OH})(\text{sal-Et})_8(\text{MeOH})]$ ( <b>8</b> )	240	84	34	20	2	9	12	5	2
23		220	48	27	8	<1	3	6	3	1
24		200	20	10	6	<1	<1	3	1	<1
25	$[\text{Ca}_4\text{K}(\mu_5\text{-OH})(\text{sal-Et})_8(\text{EtOH})]$ ( <b>9</b> )	240	70	31	12	1	7	9	7	3
26		220	28	15	5	<1	2	2	4	<1
27		200	7	4	1	0	<1	1	1	0
28	$[\text{Li}_6(\text{sal-Me})_6]$ ( <b>10</b> )	240	84	33	19	2	9	13	5	3
29		220	64	32	13	1	4	12	2	<1
30		200	41	20	11	<1	1	7	2	0
31	$[\text{Na}_6(\text{sal-Me})_6]$ ( <b>11</b> )	240	72	32	14	1	7	12	4	2
32		220	56	32	10	<1	3	10	1	<1
33		200	20	10	6	<1	<1	3	1	<1
34	$[\text{K}_6(\text{sal-Me})_6]$ ( <b>12</b> )	240	92	42	18	2	9	13	6	2
35		220	48	26	9	<1	3	8	2	<1
36		200	27	14	7	<1	1	4	1	0
37	$[\text{Mg}_2(\text{sal-Et})_4(\text{EtOH})_2]$ ( <b>13</b> )	240	71	35	11	1	7	11	5	1
38		220	28	15	7	<1	1	3	2	<1
39		200	23	11	8	<1	1	1	2	<1
40	$[\text{Zn}_4(\text{sal-Me})_8]$ ( <b>14</b> )	240	75	36	12	1	7	12	6	1
41		220	42	23	9	<1	3	1	6	<1
42		200	39	23	9	<1	1	2	4	0
43	$[\text{Mg}_2\text{Li}_2(\text{sal-Me})_6]$ ( <b>15</b> )	240	97	43	18	2	10	13	7	4
44		220	49	24	12	<1	4	7	2	<1
45		200	14	6	5	<1	1	2	<1	<1
46	$[\text{Mg}_2\text{Na}_2(\text{sal-Me})_6(\text{THF})_4]$ ( <b>16</b> )	240	98	44	18	2	10	16	5	3
47		220	51	24	11	1	4	8	2	1
48		200	21	10	6	<1	1	4	<1	<1

No.	Catalyst	T [°C]	C [%]	I [%]	II [%]	III [%]	IV [%]	V [%]	VI [%]	VII [%]
49	$[\text{Mg}_2\text{K}_2(\text{sal-Me})_6(\text{THF})_4]$ ( <b>17</b> )	240	86	41	15	1	8	14	5	2
50		220	51	25	12	<1	3	8	3	<1
51		200	39	19	13	<1	1	3	2	1
52	$[\text{Li}_2\text{Zn}_2(\text{sal-Me})_6]$ ( <b>18</b> )	240	96	39	20	2	10	13	8	4
53		220	69	34	14	1	6	9	4	1
54		200	10	6	2	<1	<1	1	1	0
55	$[\text{Na}_2\text{Zn}_2(\text{sal-Me})_6(\text{THF})_2]$ ( <b>19</b> )	240	97	38	23	2	10	10	10	4
56		220	64	35	10	1	5	8	4	1
57		200	10	5	3	<1	<1	1	1	0
58	$[\text{K}_2\text{Zn}_2(\text{sal-Me})_6(\text{THF})_2]$ ( <b>20</b> )	240	88	38	15	2	9	13	8	3
59		220	60	35	8	<1	5	7	4	1
60		200	50	27	13	1	2	2	5	0
61	$[\text{Mg}_4\text{Na}_2(\text{sal-Me})_6(\text{sal})_2(\text{THF})_4]$ ( <b>21</b> )	240	75	31	16	1	8	10	6	3
62		220	50	25	10	<1	4	9	2	<1
63		200	5	3	1	0	<1	1	<1	0

<sup>a</sup>Alcoholysis conditions:  $[\text{PA6}] = 0.48 \text{ mol/dm}^3$ ;  $[\text{catalyst}] = 0.024 \text{ mol/dm}^3$ ;  $V = 9.2 \text{ cm}^3$  of methanol. Reactions were performed using pressure reactors with a capacity of 25 mL, with reactant stoichiometry  $[\text{PA6}]/[\text{MeOH}]/[\text{M}/\text{M}'] = 1/50/0.05$ , under autogenous pressure, at 200 to 240 °C for 8 hours.

**Table S6.** Summary of alcoholysis of PA6, using methanol in the presence of **2-21** at 220 °C after 48h.<sup>a</sup>

No.	Catalyst	C [%]	I [%]	II [%]	III [%]	IV [%]	V [%]	VI [%]	VII [%]
1	catalyst-free	79	28	20	3	6	7	11	4
2	[Ca <sub>3</sub> (sal-Me) <sub>6</sub> (MeOH) <sub>2</sub> ] ( <b>2</b> )	92	35	21	3	7	7	15	4
3	[Ca <sub>2</sub> Li <sub>2</sub> (sal-Me) <sub>6</sub> (THF) <sub>2</sub> ] ( <b>3</b> )	99	30	27	6	5	3	21	7
4	[Ca <sub>2</sub> Na <sub>2</sub> (sal-Me) <sub>6</sub> (MeOH) <sub>4</sub> ] ( <b>4</b> )	97	31	23	5	6	4	21	7
5	[Ca <sub>2</sub> K <sub>2</sub> (sal-Me) <sub>6</sub> (MeOH) <sub>4</sub> ] ( <b>5</b> )	98	35	23	4	7	4	19	6
6	[CaLi <sub>6</sub> (sal-Me) <sub>8</sub> ] ( <b>6</b> )	99	32	24	5	6	15	10	7
7	[Ca <sub>3</sub> Na <sub>4</sub> (sal-Et) <sub>10</sub> (Hsal-Et) <sub>2</sub> ] ( <b>7</b> )	98	31	25	4	7	14	10	7
8	[Ca <sub>4</sub> Na(μ <sub>5</sub> -OH)(sal-Et) <sub>8</sub> (MeOH)] ( <b>8</b> )	99	26	29	6	6	16	9	7
9	[Ca <sub>4</sub> K(μ <sub>5</sub> -OH)(sal-Et) <sub>8</sub> (EtOH)] ( <b>9</b> )	97	32	21	4	6	16	11	7
10	[Li <sub>6</sub> (sal-Me) <sub>6</sub> ] ( <b>10</b> )	100	31	27	6	5	1	22	8
11	[Na <sub>6</sub> (sal-Me) <sub>6</sub> ] ( <b>11</b> )	100	30	30	5	6	2	20	7
12	[K <sub>6</sub> (sal-Me) <sub>6</sub> ] ( <b>12</b> )	97	34	25	4	7	3	17	7
13	[Mg <sub>2</sub> (sal-Et) <sub>4</sub> (EtOH) <sub>2</sub> ] ( <b>13</b> )	97	34	25	4	7	6	15	6
14	[Zn <sub>4</sub> (sal-Me) <sub>8</sub> ] ( <b>14</b> )	99	35	20	4	8	18	9	5
15	[Mg <sub>2</sub> Li <sub>2</sub> (sal-Me) <sub>6</sub> ] ( <b>15</b> )	97	30	25	5	6	15	10	6
16	[Mg <sub>2</sub> Na <sub>2</sub> (sal-Me) <sub>6</sub> (THF) <sub>4</sub> ] ( <b>16</b> )	97	30	25	5	7	15	8	7
17	[Mg <sub>2</sub> K <sub>2</sub> (sal-Me) <sub>6</sub> (THF) <sub>4</sub> ] ( <b>17</b> )	96	31	23	5	6	15	10	6
18	[Li <sub>2</sub> Zn <sub>2</sub> (sal-Me) <sub>6</sub> ] ( <b>18</b> )	98	32	25	5	6	4	19	7
19	[Na <sub>2</sub> Zn <sub>2</sub> (sal-Me) <sub>6</sub> (THF) <sub>2</sub> ] ( <b>19</b> )	97	27	26	6	5	1	25	8
20	[K <sub>2</sub> Zn <sub>2</sub> (sal-Me) <sub>6</sub> (THF) <sub>2</sub> ] ( <b>20</b> )	97	27	26	6	5	1	25	8
21	[Mg <sub>4</sub> Na <sub>2</sub> (sal-Me) <sub>6</sub> (sal) <sub>2</sub> (THF) <sub>4</sub> ] ( <b>21</b> )	96	29	27	5	7	3	18	7

<sup>a</sup> Alcoholysis conditions: [PA6] = 0.48 mol/dm<sup>3</sup>; [catalyst] = 0.024 mol/dm<sup>3</sup>; V = 9.2 cm<sup>3</sup> of methanol. Reactions were performed using pressure reactors with a capacity of 25 mL, with reactant stoichiometry [PA6]/[MeOH]/[M/M'] = 1/50/0.05, under autogenous pressure, through 48 h at 220 °C.

**Table S7.** Summary of PA6 alcoholysis using BnOH and **12** as catalyst after 6 - 54 h at 220 – 260 °C.

No.	[PA6]/[BnOH]	T [°C]	t [h]	I [%]	II [%]	III [%]	IV [%]	IV' [%]
1	1/10	220	25	47	12	11	24	6
2	1/10	260	6	34	23	17	19	7
3	1/10	260	29	9	6	24	55	5
4	1/10	260	54	2	9	26	56	7

<sup>a</sup> Alcoholysis conditions: [PA6] = 0.96 mol/dm<sup>3</sup>; [M/M'] = 0.047 mol/dm<sup>3</sup>; V = 4.6 cm<sup>3</sup> of benzyl alcohol. Reactions were performed using pressure reactors with a capacity of 25 mL, with reactant stoichiometry [PA6]/[BnOH]/[M'] = 1/10/0.05, under autogenous pressure, through 6-54h at 220 - 260 °C.

**Table S8.** Summary of PA6 alcoholysis using BnOH and **2-6** and **10-21** as catalysts at 260 °C after 8 hours.<sup>a</sup>

No.	Catalyst	I [%]	II [%]	III [%]	IV [%]	IV' [%]
1	catalyst free	30	20	20	19	11
2	[Ca <sub>3</sub> (sal-Me) <sub>6</sub> (MeOH) <sub>2</sub> ] ( <b>2</b> )	45	17	7	19	12
3	[Ca <sub>2</sub> Li <sub>2</sub> (sal-Me) <sub>6</sub> (THF) <sub>2</sub> ] ( <b>3</b> )	52	8	15	19	6
4	[Ca <sub>2</sub> Na <sub>2</sub> (sal-Me) <sub>6</sub> (MeOH) <sub>4</sub> ] ( <b>4</b> )	61	4	10	19	6
5	[Ca <sub>2</sub> K <sub>2</sub> (sal-Me) <sub>6</sub> (MeOH) <sub>4</sub> ] ( <b>5</b> )	58	11	10	14	7
6	[CaLi <sub>6</sub> (sal-Me) <sub>8</sub> ] ( <b>6</b> )	46	6	11	32	5
7	[Li <sub>6</sub> (sal-Me) <sub>6</sub> ] ( <b>10</b> )	39	12	11	36	2
8	[Na <sub>6</sub> (sal-Me) <sub>6</sub> ] ( <b>11</b> )	21	25	21	25	8
9	[K <sub>6</sub> (sal-Me) <sub>6</sub> ] ( <b>12</b> )	37	14	16	24	9
10	[Mg <sub>2</sub> (sal-Et) <sub>4</sub> (EtOH) <sub>2</sub> ] ( <b>13</b> )	23	6	26	42	3
11	[Zn <sub>4</sub> (sal-Me) <sub>8</sub> ] ( <b>14</b> )	36	17	18	18	11
12	[Mg <sub>2</sub> Li <sub>2</sub> (sal-Me) <sub>6</sub> ] ( <b>15</b> )	64	7	10	14	5
13	[Mg <sub>2</sub> Na <sub>2</sub> (sal-Me) <sub>6</sub> (THF) <sub>4</sub> ] ( <b>16</b> )	66	3	11	15	5
14	[Mg <sub>2</sub> K <sub>2</sub> (sal-Me) <sub>6</sub> (THF) <sub>4</sub> ] ( <b>17</b> )	61	2	13	20	4
15	[Li <sub>2</sub> Zn <sub>2</sub> (sal-Me) <sub>6</sub> ] ( <b>18</b> )	52	8	17	17	6
16	[Na <sub>2</sub> Zn <sub>2</sub> (sal-Me) <sub>6</sub> (THF) <sub>2</sub> ] ( <b>19</b> )	49	8	20	16	7
17	[K <sub>2</sub> Zn <sub>2</sub> (sal-Me) <sub>6</sub> (THF) <sub>2</sub> ] ( <b>20</b> )	51	9	10	22	8
18	[Mg <sub>4</sub> Na <sub>2</sub> (sal-Me) <sub>6</sub> (sal) <sub>2</sub> (THF) <sub>4</sub> ] ( <b>21</b> )	44	11	20	20	5

<sup>a</sup> Alcoholysis conditions: [PA6] = 0.96 mol/dm<sup>3</sup>; [M/M'] = 0.047 mol/dm<sup>3</sup>; V = 4.6 cm<sup>3</sup> of benzyl alcohol. Reactions were performed using pressure reactors with a capacity of 25 mL, with reactant stoichiometry [PA6]/[BnOH]/[M/M'] = 1/10/0.05, under autogenous pressure, through 8h at 260 °C.

## Literature

<sup>1</sup> M. Y. Kondo, L. S. Montagna, G. F. De Melo Morgado, A. L. G. De Castilho, L. A. P. D. S. Batista, E. C. Botelho, M. L. Costa, F. R. Passador, M. C. Rezende and M. V. Ribeiro, Recent advances in the use of Polyamide-based materials for the automotive industry, *Polímeros*, 2022, **32**, e2022023.

<sup>2</sup> V. Hirschberg and D. Rodrigue, Recycling of polyamides: Processes and conditions, *J. Polym. Sci.*, 2023, **61**, 1937–1958.

<sup>3</sup> P. P. X. Yap, Z. Yen, T. Salim, H. C. A. Lim, C. K. Chung and Y. M. Lam, The impact of mechanical recycling on the degradation of polyamide, *Polym. Degrad. Stab.*, 2024, **225**, 110773.

- 
- <sup>4</sup> A.-J. Minor, R. Goldhahn, L. Rihko-Struckmann and K. Sundmacher, Chemical recycling processes of nylon 6 to Caprolactam: review and Techno-Economic assessment, *J. Chem. Eng.*, 2023, **474**, 145333.
- <sup>5</sup> A. McNeeley and Y. A. Liu, Assessment of Nylon-6 depolymerization for circular economy: kinetic modeling, purification, sustainable process design, and industrial practice, *Ind. Eng. Chem. Res.*, 2024, **63**, 16953–16989.
- <sup>6</sup> A. Kamimura, K. Ikeda, S. Suzuki, K. Kato, Y. Akinari, T. Sugimoto, K. Kashiwagi, K. Kaiso, H. Matsumoto and M. Yoshimoto, Efficient conversion of polyamides to  $\Omega$ -Hydroxyalkanoic acids: a new method for chemical recycling of waste plastics, *ChemSusChem*, 2014, **7**, 2473–2477.
- <sup>7</sup> Z. Liu and Y. Ma, Chemical recycling of Step-Growth polymers guided by Le Chatelier's principle, *ACS Eng. Au*, 2024, **4**, 432–449.
- <sup>8</sup> C. Mihut, D. K. Captain, F. Gadala-Maria and M. D. Amiridis, Review: Recycling of nylon from carpet waste, *Polym. Eng. Sci.*, 2001, **41**, 1457–1470.
- <sup>9</sup> M. L. Zheng, M. Wang, Y. Li, Y. Xiong and C. Wu, Recycling and degradation of polyamides, *Molecules*, 2024, **29**, 1742.
- <sup>10</sup> S. Czernik, C. C. Elam, R. J. Evans, R. R. Meglen, L. Moens and K. Tatsumoto, Catalytic pyrolysis of nylon-6 to recover caprolactam, *J. Anal. Appl. Pyrolysis*, 1998, **46**, 51–64.
- <sup>11</sup> A. K. Mukherjee and D. K. Goel, Depolymerization of poly- $\epsilon$ -caprolactam catalyzed by sodium hydroxide, *J. Appl. Polym. Sci.*, 1978, **22**, 361–368.
- <sup>12</sup> L. Wursthorn, K. Beckett, J. O. Rothbaum, R. M. Cywar, C. Lincoln, Y. Kratish and T. J. Marks, Selective Lanthanide-Organic catalyzed depolymerization of nylon-6 to E-Caprolactam, *Angew. Chem.*, 2023, **62**, e202212543.
- <sup>13</sup> A. Kamimura and S. Yamamoto, *Org. Lett.*, 2007, **9**, 2533–2535.
- <sup>14</sup> Y. Iwasaki, T. Kawakita and S.-I. Yusa, Thermoresponsive polyphosphoesters bearing enzyme-cleavable side chains, *Chem. Lett.*, 2009, **38**, 1054–1055.
- <sup>15</sup> S. Sifniades, A. B. Levy, J. A. J. Hendrix, WO Pat., 9720813, 1997, AlliedSignal Inc. (CAN: 127:82490).
- <sup>16</sup> T. F. Corbin, E. A. Davis, J. A. Dellinger, US Pat., 5169870, 1992, BASF Corp. (CAN: 118:81671).
- <sup>17</sup> R. Kotek, US Pat., 5294707, 1994, BASF Corp. (CAN 120:246113).

- 
- <sup>18</sup> H. Hu, Q. Xu, L. Sun, R. Zhu, T. Gao, Y. He, B. Ma, J. Yu and X. Wang, Rapid hydrolysis of waste and scrap PA6 textiles to E-Caprolactam, *ACS Appl. Polym. Mater.*, 2023, **5**, 751–763.
- <sup>19</sup> U. Klun, Rapid microwave induced depolymerization of polyamide-6, *Polymer*, 2000, **41**, 4361–4365.
- <sup>20</sup> C. Alberti, R. Figueira, M. Hofmann, S. Koschke and S. Enthaler, Chemical recycling of End-of-Life polyamide 6 via ring closing depolymerization, *ChemistrySelect*, 2019, **4**, 12638–12642.
- <sup>21</sup> R. J. McKinney, US Pat., 5302756, 1994, du Pont de Nemours, E. I., and Co. (CAN 121:109987).
- <sup>22</sup> J. A. J. Hendrix, M. Booij, Y. H. Frentzen, EP Pat., 737666, 1996, Dsm N.V. (CAN 125:330815).
- <sup>23</sup> A. Kumar, N. Von Wolff, M. Rauch, Y.-Q. Zou, G. Shmul, Y. Ben-David, G. Leitus, L. Avram and D. Milstein, Hydrogenative depolymerization of nylons, *J. Am. Chem. Soc.*, 2020, **142**, 14267–14275.
- <sup>24</sup> B. Hommez and E. J. Goethals, Degradation of nylon-6 by glycolysis. Part 1: Identification of degradation products, *J. Macromol. Sci., Part A*, 1998, **35**, 1489–1505.
- <sup>25</sup> A. Kamimura, Y. Oishi, K. Kaiso, T. Sugimoto and K. Kashiwagi, Supercritical Secondary Alcohols as Useful Media To Convert Polyamide into Monomeric Lactams, *ChemSusChem*, 2007, **1**, 82–84.
- <sup>26</sup> A. Kamimura, K. Kaiso, S. Suzuki, Y. Oishi, Y. Ohara, T. Sugimoto, K. Kashiwagi and M. Yoshimoto, Direct conversion of polyamides to  $\omega$ -hydroxyalkanoic acid derivatives by using supercritical MeOH, *Green Chem.*, 2011, **13**, 2055–2061.